

Quantum Kinetic Theory for Quantum Electrodynamics

Shu Lin *

School of Physics and Astronomy, Sun Yat-Sen University, Zhuhai 519082, China

November 2, 2021

Abstract

We derive a quantum kinetic theory for QED including both elastic and inelastic collisions with screening effect. By assuming parity invariance, we find the classical limit of the kinetic theory generalizes the well-known classical kinetic theory to massive case. The resulting classical kinetic theory simplifies when fermion bare mass is much greater than thermal mass. In this case only elastic collision is relevant and screening is only needed for Coulomb scattering. For a given solution to the classical kinetic theory, we find at $O(\hbar)$ non-dynamical part of the quantum correction to Wigner functions for fermion and photon, which gives rise to spin polarization for fermion and photon respectively. Other contributions to spin polarizations from dynamical part of the correction to Wigner function are possible when parity violating sources are present.

*linshu8@mail.sysu.edu.cn

1 Introduction and Summary

Spin polarization phenomena have been observed in a variety of experiments in particle physics [1–3] and condensed matter physics [4, 5]. It can be induced by different sources such as electromagnetic field [6, 7], vorticity [8–11]. In order to describe spin transports in a non-equilibrium setting, two complementary frameworks have been developed. One is spin kinetic theory [12–16], which generalizes the chiral kinetic theory [17–35] to massive case. The spin kinetic theory is organized as a systematic expansion in \hbar , with the zeroth order gives the classical kinetic theory and spin effect appears from the first order. On general ground, one expects the zeroth order kinetic theory reduces to the classical Boltzmann equations written down by Arnold, Moore and Yaffe (AMY) [36–38] for quantum chromodynamics (QCD), which is essentially spin-averaged kinetic equations. Recently much progress has been made towards realistic collisions term for the spin kinetic theory [22, 39–44, 44–50]. However a complete derivation of realistic collision term for QCD has yet to be performed.

The other framework is spin hydrodynamics [51–63], which includes spin density as an additional degree of freedom in conventional hydrodynamics. It is assumed that the spin density relaxes much slower than the other non-hydrodynamic modes. The assumption clearly depends on particular microscopic theory. It is desirable to confirm that such an assumption is indeed satisfied in systems of our interest.

In this paper, we derive quantum kinetic equations for quantum electrodynamics (QED) as a prototype of QCD. It is known that for massive fermion, the kinetic theory contains the following degrees of freedom: f_V^e/f_A^e , a_μ being vector/axial charge distribution functions and spin direction respectively [12]. By assuming the system is parity invariant, we are left with f_V^e (to be denoted as f_e) as the only degree of freedom. A similar reduction applies to the photonic sector of kinetic theory, leaving only the distribution function of unpolarized photon f_γ as the degree of freedom. With these simplifications, we derive a quantum kinetic theory, which to the lowest order in \hbar generalizes the classical kinetic theory by AMY [36–38] to massive case for QED. It has all the ingredients of the classical Boltzmann equations, including both $2 \leftrightarrow 2$ elastic and $1 \leftrightarrow 2$ inelastic collisions. The screening effect is automatically taken into account. We discuss two representative scenarios for the fermion mass m : $m \gg e\Lambda$ and $m \lesssim e\Lambda$, with Λ being a characteristic scale for momenta. In the former scenarios, inelastic collisions are not relevant, and screening is only needed for elastic Coulomb scattering. The latter scenario is formally similar to [36–38].

It is informative to compare the classical kinetic theories for QED and QCD. On one hand, they share similar scales: characteristic momentum of quasi-particles Λ ; ther-

mal/screening mass $e\Lambda(g\Lambda)$; damping rate of quasi-particles $e^2\Lambda(g^2\Lambda)$ and mean-free time $\frac{1}{e^4\Lambda} \left(\frac{1}{g^4\Lambda} \right)$. On the other hand, they differ in one fundamental aspect: QED does not possess a non-perturbative scale while QCD does. The non-perturbative scale for QCD cuts off long range fluctuation of chromoelectromagnetic fields, allowing for omission fluctuation of chromoelectromagnetic fields beyond the scale $\frac{1}{e^2\Lambda}$. However such a mechanism is not present in QED. We will instead choose a larger coarse-graining scale $1/e^4\Lambda$ for the kinetic theory and restrict ourselves to the situation without background electromagnetic fields. Moreover, we will show electromagnetic fields generated by fluctuations at the scale $\frac{1}{e^4\Lambda}$ have a subleading effect as compared to that of spacetime gradients.

The classical kinetic theory from the lowest order expansion in \hbar provides a realistic background, on which we can do systematic quantum correction. The next order expansion in \hbar gives rise to a quantum kinetic theory for describing the spin polarization effects as well as studying spin transports for QED system. Given a solution to the classical kinetic equations for arbitrary source, we find part of the quantum correction to the solution at $O(\hbar)$. This part is determined from constraint equations thus is non-dynamical. The dynamical part will have to be determined by quantum corrections to the collision term. When parity violating sources are present, additional contribution to spin polarization at $O(\hbar)$ may be generated dynamically. Further analysis is left for future studies.

The paper is organized as follows: in Section 2, we derive the Kadanoff-Baym equations for fermions and photons. By the assumption of parity invariance, the degrees of freedom are identified as unpolarized fermion/photon distribution functions. We also discuss regimes of validity of the kinetic theory; in Sections 3 and 4, we elaborate on the self-energies of fermions and photons, which gives rise to the elastic and inelastic collision terms. In order to incorporate the interference term in $2 \leftrightarrow 2$ process and $1 \leftrightarrow 2$ process, it is crucial to include vertex correction in the self-energies. The resulting kinetic theory has close resemblance to the Boltzmann equations by AMY; in Section 5, we find the non-dynamical quantum correction to the solutions for fermion/photon at $O(\hbar)$, for a given solution to the classical kinetic equations; we provide outlook in Section 6.

2 Kadanoff-Baym Equations for QED

2.1 Fermionic Kadanoff-Baym Equations

We begin by writing down the fermionic part of the Lagrangian

$$\frac{\mathcal{L}}{\hbar} = \bar{\psi} \left(i\cancel{\partial} - e\cancel{A} - \frac{m}{\hbar} \right) \psi + \bar{\eta}\psi + \bar{\psi}\eta, \quad (1)$$

where $\bar{\eta}$ and η are sources coupled to ψ and $\bar{\psi}$ respectively. We first write down the Dyson-Schwinger equation on the Schwinger-Keldysh (SK) contour

$$\left(i\cancel{\partial}_x - \frac{m}{\hbar} \right) \psi(x) = \eta(x) + \eta_{\text{ind}}(x), \quad (2)$$

$$\bar{\psi}(y) \left(-i\overleftarrow{\cancel{\partial}}_y - \frac{m}{\hbar} \right) = \bar{\eta}(y) + \bar{\eta}_{\text{ind}}(y), \quad (3)$$

with $\eta_{\text{ind}} = e\cancel{A}\psi$ and $\bar{\eta}_{\text{ind}} = e\bar{\psi}\cancel{A}$ ¹. For simplicity, we have assumed the absence of background gauge field. Following [65], we take the derivative $i\frac{\delta}{\delta\eta(y)}$ on (2) to obtain

$$\left(i\cancel{\partial}_x - \frac{m}{\hbar} \right) S_c(x, y) = i\delta_c(x - y) + i\frac{\eta_{\text{ind}}(x)}{\eta(y)}, \quad (4)$$

where the subscript indicates the quantity being contour-time ordered. The matrix form of $S_c(x, y)$ in 12 basis is given by

$$S_{c, \alpha\beta}(x, y) = \begin{pmatrix} S_{\alpha\beta}^{11}(x, y) & S_{\alpha\beta}^{<}(x, y) \\ S_{\alpha\beta}^{>}(x, y) & S_{\alpha\beta}^{22}(x, y) \end{pmatrix} = \begin{pmatrix} \langle T\psi_\alpha(x)\bar{\psi}_\beta(y) \rangle & -\langle \bar{\psi}_\beta(y)\psi_\alpha(x) \rangle \\ \langle \psi_\alpha(x)\bar{\psi}_\beta(y) \rangle & \langle \bar{T}\psi_\alpha(x)\bar{\psi}_\beta(y) \rangle \end{pmatrix}. \quad (5)$$

We have also kept explicit Dirac indices $\alpha\beta$ in (5). T and \bar{T} correspond to time ordering and anti-time ordering. The last term of (4) can be evaluated as

$$\frac{\delta}{\delta\eta(y)}\eta_{\text{ind}}(x) = \int d^4z \left(-i\frac{\delta}{\delta\psi(z)}\eta_{\text{ind}}(x) \right) \left(i\frac{\delta}{\delta\eta(y)}\delta\psi(z) \right) = \int d^4z \Sigma_c(x, z) S_c(z, y), \quad (6)$$

with $\Sigma_c(x, y) = -i\frac{\delta}{\delta\psi(y)}\eta_{\text{ind}}(x) = \langle \eta_{\text{ind}}(x)\bar{\eta}_{\text{ind}}(y) \rangle_c$. Taking x and y on the forward and backward contours respectively, we obtain

$$\left(i\cancel{\partial}_x - \frac{m}{\hbar} \right) S^{<}(x, y) = i \int d^4z \Sigma_F(x, z) S^{<}(z, y) - i \int d^4z \Sigma^{<}(x, z) S_{\bar{F}}(z, y). \quad (7)$$

We can eliminate the time ordered self-energy Σ_F and anti-time ordered correlator $S_{\bar{F}}$ in favor of retarded/advanced correlator defined as

$$\begin{aligned} S_R(x, y) &= i\theta(x_0 - y_0) (S^{>}(x, y) - S^{<}(x, y)) \\ S_A(x, y) &= -i\theta(y_0 - x_0) (S^{>}(x, y) - S^{<}(x, y)), \end{aligned}$$

¹Recall the dimensions of fields: $\psi \sim \text{length}^{-3/2}$, $A \sim \text{length}^{-1}$. By writing down the vertex in (1), we have redefined the coupling constant e such that it contains no factor of \hbar .

and similar definitions for $\Sigma_{R/A}$. Using the following relations

$$\begin{aligned}\Sigma_F(x, z) &= -i\Sigma_R(x, z) + \Sigma^<(x, z) \\ S_{\bar{F}}(z, y) &= S^<(z, y) + iS_A(z, y),\end{aligned}\tag{8}$$

we arrive at the standard form of KB equations for fermions

$$\left(i\phi_x - \frac{m}{\hbar}\right) S^<(x, y) = \int d^4z \left(\Sigma_R(x, z)S^<(z, y) + \Sigma^<(x, z)S_A(z, y)\right).\tag{9}$$

We will rewrite (9) in terms of Wigner transformed lesser propagator

$$\tilde{S}^<(X = \frac{x+y}{2}, P) = \int d^4(x-y) e^{iP \cdot (x-y)/\hbar} \langle S^<(x, y) \rangle.\tag{10}$$

The RHS can be expressed using $\tilde{S}^<(X, P)$ and counterpart for self-energy by the following expansion

$$\int d^4z A(x, z)B(z, y) = \int_K e^{-iK \cdot (x-y)} \left(\tilde{A}\tilde{B} + \frac{i\hbar}{2}\{\tilde{A}, \tilde{B}\}_{\text{PB}}\right) + O(\hbar^2),\tag{11}$$

where the Poisson bracket is defined as

$$\{\tilde{A}, \tilde{B}\} = \partial_k \tilde{A} \cdot \partial_X \tilde{B} - \partial_X \tilde{A} \cdot \partial_k \tilde{B},\tag{12}$$

and $\int_K \equiv \int \frac{d^4K}{(2\pi)^4}$. The Wigner transform of (9) then reads

$$\frac{i}{2}\phi S^< + \frac{\not{P} - m}{\hbar} S^< = (\Sigma_R S^< + \Sigma^< S_A) + \frac{i\hbar}{2} (\{\Sigma_R, S^<\}_{\text{PB}} + \{\Sigma^<, S_A\}_{\text{PB}}).\tag{13}$$

We have dropped the tildes and the common arguments (X, P) for propagators and self-energies for notational simplicity.

To proceed further, we use the quasi-particle approximation [65], in which the spectral density is given by

$$\rho(X, P) = S^>(X, P) - S^<(X, P) = 2\pi\hbar\epsilon(p_0) (\not{P} + m) \delta(P^2 - m^2 - 2P^\mu Re\Sigma_\mu^R),\tag{14}$$

where $\epsilon(p_0)$ is the sign function and $\Sigma_\mu^R = \frac{1}{4}tr[\gamma_\mu \Sigma^R]$. The structure of (14) indicates quasi-particle has a momentum shifted by $Re\Sigma_\mu^R$ and has a vanishing damping rate $\Gamma(X, P)$. For system with characteristic momenta Λ , $Re\Sigma^R \sim e\Lambda$ and damping rate $\sim e^2\Lambda$. We can indeed ignore $Re\Sigma_\mu^R$ next to P_μ and Γ . We can use the following representations to further simplify (13)²

$$\begin{aligned}\Sigma^R &= Re\Sigma^R + \frac{i}{2}(\Sigma^> - \Sigma^<) \\ S^A &= ReS^R - \frac{i}{2}(S^> - S^<),\end{aligned}$$

²The real part is formally defined with hermitian conjugate as $ReA = \frac{1}{2}(A + \gamma^0 A^\dagger \gamma^0)$.

and ignore $Re\Sigma^R$ and $ReS^R \propto \Gamma$ as reasoned above to arrive at

$$\frac{i}{2}\not{\partial}S^< + \frac{\not{P} - m}{\hbar}S^< = \frac{i}{2}(\Sigma^>S^< - \Sigma^<S^>) - \frac{\hbar}{4}(\{\Sigma^>, S^<\}_{\text{PB}} + \{\Sigma^<, S^>\}_{\text{PB}}). \quad (15)$$

(15) can be solved order by order in \hbar

$$S^< = S^{<(0)} + \hbar S^{<(1)} + \dots, \quad (16)$$

with the lowest order solution given by [12]

$$S^{<(0)} = -2\pi\hbar\epsilon(P \cdot u)\delta(P^2 - m^2) \left((\not{P} + m)f_V^e + \gamma^5\not{u}f_A^e - \frac{\sigma^{\mu\nu}\epsilon_{\mu\nu\rho\sigma}P^\rho a^\sigma}{2m}f_A^e \right). \quad (17)$$

Note that we have introduced an observer's frame vector u in the sign function, which separates particles and anti-particles. Despite appearance of u , it is actually frame independent at this order because boosts do not change a particle into anti-particle. f_V^e/f_A^e and a^μ correspond to vector/axial distributions and spin direction vector respectively. We will assume that the system is parity invariant, which means $f_A^e = 0$, leaving f_V^e as the only degree of freedom.³ This is identified as fermion distribution function in classical kinetic theory. We will denote f_V^e as f_e below. The lowest order solution can be written as

$$S^{<(0)}(X, P) = -2\pi\hbar\epsilon(P \cdot u)\delta(P^2 - m^2)(\not{P} + m)f_e(X, P), \quad (18)$$

which is nothing but the equilibrium fermion propagator with Fermi-Dirac distribution promoted to spacetime dependent distribution f_e .

In fact f_e satisfies the constraint $f_e(X, P) + f_e(X, -P) = 1$ like Fermi-Dirac distribution. To see the origin of the constraint, we can show from the definition (5) that $\text{tr}[S^<(x, y)] = -\text{tr}[S^>(y, x)]$, which gives $\text{tr}[S^<(X, P)] = -\text{tr}[S^>(X, -P)]$. Combining with (18), we easily arrive at the constraint. Furthermore, we have the following property

$$S^{>(0)}(X, -P, m) = S^{<(0)}(X, P, -m). \quad (19)$$

Defining

$$\bar{S}^{>/<(0)}(X, P, m) = S^{>/<(0)}(X, P, -m), \quad (20)$$

we can then write down the following useful relations

$$\bar{S}^{<(0)}(X, P, m) = S^{>(0)}(X, -P, m), \quad (21)$$

³It is parity invariant in the sense that there is no difference between distributions of opposite chiral components and similarly for photons. However, in an out-of-equilibrium setting sources with both parities such as spacetime gradient of temperature and fluid velocity etc.

and a similar one with $\rangle \leftrightarrow \langle$. Below S and \bar{S} always contain the argument m , which we omit from now. (21) suggests the interpretation of $\bar{S}^{\rangle/\langle(0)}$ as charge-conjugated Wigner function: when $S^{\langle(0)}(X, P)$ describes particles, $\bar{S}^{\rangle(0)}(X, P)$ describes anti-particle and vice versa.

2.2 Photonic Kadanoff-Baym Equations

We now turn to the photonic counterpart starting with the following relevant part of the Lagrangian

$$\frac{\mathcal{L}}{\hbar} = -\frac{1}{4}F_{\mu\nu}^2 + \bar{\psi}(-eA_\mu)\psi - A_\mu j^\mu - \frac{1}{2\xi} \left(P^{\alpha\beta} \partial_\alpha A_\beta \right)^2, \quad (22)$$

where j^μ is the source to A_μ . The last term is the gauge fixing term for Coulomb gauge, with the projector $P^{\alpha\beta}$ defined with an observer's frame vector n^α as: $P^{\alpha\beta} = n^\alpha n^\beta - g^{\alpha\beta}$. We will take n^μ to be the same frame vector as the fermionic one u^μ . It projects out the temporal component of a vector. The Coulomb gauge singles out transversely polarized photon as the physical degrees of freedom, offering a quick path to kinetic theory.

The Dyson-Schwinger equation for photon is given by

$$\left(\partial^2 g^{\mu\nu} - \partial^\mu \partial^\nu \right) A_\nu(x) + \frac{1}{\xi} \left(P^{\mu\nu} \partial_\nu P^{\alpha\beta} \partial_\alpha A_\beta(x) \right) = j^\mu(x) + j_{\text{ind}}^\mu(x), \quad (23)$$

where $j_{\text{ind}}^\mu = \bar{\psi} \gamma^\mu \psi$. Taking the derivative $i \frac{\delta}{\delta j^\rho(y)}$ on the SK-contour, we obtain

$$\left(\partial^2 g^{\mu\nu} - \partial^\mu \partial^\nu + \frac{1}{\xi} P^{\mu\alpha} P^{\nu\beta} \partial_\alpha \partial_\beta \right)_x D_{\nu\rho}^c(x, y) = i \delta_\rho^\mu \delta_c(x - y) + i \int d^4 z \Pi_c^{\mu\nu}(x, z) D_{\nu\rho}^c(z, y), \quad (24)$$

where $D_{\nu\rho}^c(x, y) = \langle A_\nu(x) A_\rho(y) \rangle_c$ and $\Pi_c^{\mu\nu}(x, y) = \langle j_{\text{ind}}^\mu(x) j_{\text{ind}}^\nu(y) \rangle_c$. The subscript x indicates the derivatives acting on x . The usual Coulomb gauge is recovered in the limit $\xi \rightarrow 0$:

$$P^{\mu\alpha} \partial_\alpha D_{\mu\nu}^<(x, y) = 0. \quad (25)$$

Following similar procedures as the fermionic case for the Wigner transform and quasi-particle approximation, we arrive at

$$\begin{aligned} & \left[\frac{1}{\hbar^2} \left(-P^2 g^{\mu\nu} + P^\mu P^\nu - \frac{1}{\xi} P^{\mu\alpha} P^{\nu\beta} P_\alpha P_\beta \right) + \frac{i}{2\hbar} \left(-2P \cdot \partial g^{\mu\nu} + (\partial^\mu P^\nu + \partial^\nu P^\mu) \right. \right. \\ & \left. \left. - \frac{1}{\xi} P^{\mu\alpha} P^{\nu\beta} (\partial_\alpha P_\beta + \partial_\beta P_\alpha) \right) + \frac{1}{4} \left(\partial^2 g^{\mu\nu} - \partial^\mu \partial^\nu + \frac{1}{4\xi} P^{\mu\alpha} P^{\nu\beta} \partial_\alpha \partial_\beta \right) \right] D_{\nu\rho}^< = \\ & \frac{i}{2} (\Pi^{\mu\nu>} D_{\nu\rho}^< - \Pi^{\mu\nu<} D_{\nu\rho}^>) + \frac{\hbar}{4} \{ \Pi^{\mu\nu>}, D_{\nu\rho}^< \} - \frac{\hbar}{4} \{ \Pi^{\mu\nu<}, D_{\nu\rho}^> \}, \end{aligned} \quad (26)$$

with the Coulomb gauge condition

$$P^{\mu\alpha} \left(\frac{\hbar}{2} \partial_\alpha - iP_\alpha \right) D_{\mu\nu}^< = 0. \quad (27)$$

We seek solution to (26) and (27) order by order in \hbar

$$D_{\mu\nu}^< = D_{\mu\nu}^{<(0)} + \hbar D_{\mu\nu}^{<(1)} + \dots, \quad (28)$$

with the lowest order solution given by [66–68]

$$D_{\mu\nu}^{<(0)} = 2\pi\epsilon(P \cdot u) \delta(P^2) (P_{\mu\nu}^T f_V^\gamma - i S_{\mu\nu} f_A^\gamma), \quad (29)$$

where $P_{\mu\nu}^T = P_{\mu\nu} - \frac{P_{\mu\alpha} P_{\nu\beta} P^\alpha P^\beta}{(P \cdot u)^2}$ and $S_{\mu\nu} = \frac{\epsilon_{\mu\nu\rho\sigma} P^\rho u^\sigma}{P \cdot u}$ are parity even and odd projectors perpendicular to $P_{\mu\alpha} P^\alpha$. With these projectors, the Coulomb gauge condition (27) is automatically satisfied. Similar to the fermionic case, in a parity invariant system, $f_A^\gamma = 0$ and we denote f_V^γ as f_γ , which is to be identified as photon distribution function. We have then a simplified Wigner function for photon

$$D_{\mu\nu}^{<(0)}(X, P) = 2\pi\epsilon(P \cdot u) \delta(P^2) P_{\mu\nu}^T f_\gamma(X, P), \quad (30)$$

which is nothing but the equilibrium photon propagator in Coulomb gauge with Bose-Einstein distribution promoted to spacetime dependent distribution f_γ . Similar to the fermionic case, the distribution satisfies the constraint $f_\gamma(X, -P) = -1 - f_\gamma(X, P)$. It follows from

$$D_{\mu\nu}^<(x, y) = D_{\nu\mu}^>(y, x) \Rightarrow D_{\mu\nu}^{<(0)}(X, P) = D_{\nu\mu}^{>(0)}(X, -P) = D_{\mu\nu}^{>(0)}(X, -P), \quad (31)$$

upon using (30).

2.3 Classical kinetic equations and regime of validity

Now we determine the dynamics of f_e and f_γ . For the former, it is known that $S^{<(1)}$ contains only axial and tensor components [12, 42]. Taking the trace of (15), we find $\text{tr}[(\not{P} - m)S^{<(1)}] = 0$, and we arrive at

$$\text{tr}[\not{P} S^{<(0)}] = \text{tr}[\Sigma^{>(0)} S^{<(0)} - \Sigma^{<(0)} S^{>(0)}], \quad (32)$$

where $S^{<(0)}$ is given by (18).

For the latter, we assume $D_{\nu\rho}^{<(1)}$ is on-shell. The dynamics of f_γ can be derived by contracting (26) with $P_\mu^{T,\rho}$. We find $P_\mu^{T,\rho} (-P^2 g^{\mu\nu} + P^\mu P^\nu - \frac{1}{\xi} P^{\mu\alpha} P^{\nu\beta} P_\alpha P_\beta) D_{\nu\rho}^{<(1)} = 0$ at $O(\hbar^{-1})$. The remaining terms give the dynamical equation for f_γ :

$$-2P \cdot \partial g^{\mu\nu} D_{\nu\mu}^{<(0)} = \hbar \left(\Pi^{\mu\nu >(0)} D_{\nu\mu}^{<(0)} - \Pi^{\mu\nu <(0)} D_{\nu\mu}^{>(0)} \right). \quad (33)$$

The presence of \hbar in the classical kinetic equation is consistent with the dimension of photon self-energies $\Pi^{\mu\nu>/<}(X, P) \sim \text{length}^{-2}$.

In order to close the equations, we need to express $\Sigma^{</>(0)}$ and $\Pi^{\mu\nu>/<(0)}$ in terms of f_e and f_γ . This is the subject of the next two sections. As we shall see, the self-energies consistently incorporate elastic and inelastic collisions in the known classical kinetic theory. We will set $\hbar = 1$ in the next two sections, with the understanding that factors of \hbar can always be reinstated by dimension in the classical collision term. We will retain \hbar in Section 5 when we discuss quantum corrections.

Before presenting details on the self-energies, we discuss the regime of validity of the kinetic theory. The key conditions to be satisfied are the following:

- i. A separation of scales between quasi-particle momenta Λ , thermal mass $e\Lambda$ and damping rate $e^2\Lambda$;
- ii. The physical observable of our interest is dominated by the dynamics of quasi-particles, which are described by the kinetic theory;
- iii. The coordinate in the kinetic theory is coarse-grained within the scale $1/e^4\Lambda$. Collisions are local on every coarse-grained spacetime point. The coarse-graining scale will also be crucial for condition v below. The distributions are assumed not to vary significantly over the scale $1/e^4\Lambda$;
- iv. The distributions can only be weakly anisotropic such that instability associated with electromagnetic fields does not affect the dynamics of quasi-particles;
- v. A background electromagnetic field is excluded by assumption. The effect of electromagnetic fields from thermal fluctuations is negligible compared to spacetime derivatives $e|A| \ll \partial_X$. This is possible due to large conductivity of the medium, which suppresses the fluctuation of electromagnetic fields $e|A| \sim e^6\Lambda$;
- vi. Since the equations and solutions are organized by expansion in \hbar , we need to have the quantum correction small compared to the classical counterpart. This is guaranteed by $\partial_X \ll \Lambda$.

We will not elaborate on all of them because many of them are parallel to the QCD case. Below we will be more specific on iv through vi.

iv. It is known that anisotropic distribution in momentum can lead to filamentation instability, in which electromagnetic field draws energy from quasi-particles and grow exponentially [69], see [70] for a recent review. The time scale of the instability can be estimated following [71]. For a given class of anisotropic distributions $f_{\text{iso}}(\sqrt{\mathbf{p}^2 + \xi(\mathbf{p} \cdot \mathbf{n})^2})$, with ξ and n corresponding to magnitude and axis of anisotropy respectively, the unstable modes

for weakly anisotropic case $\xi \ll 1$ is found to have a characteristic frequency $\xi^{3/2}e^2T$ [71]. In order for the unstable mode not to invalidate the kinetic theory, we require the instability occurs more slowly than characteristic time scale of the kinetic theory $\xi^{3/2}eT \ll e^4T$, which leads to $\xi \ll e^2$.

v. Now we justify the omission of electromagnetic fields. While we exclude background electromagnetic fields by assumption, the latter can still be generated by thermal fluctuations. We show that their effect is subleading compared to that of spacetime derivatives. The magnitude of the fluctuation depends on the property of the medium and the time scale of the fluctuation. For simplicity, we will probe the medium in equilibrium, which is expected to give the correct parametric estimate. We will probe the medium with an external current $(\rho_{\text{ex}}, \vec{j}_{\text{ex}})$. The electromagnetic fields satisfy Maxwell equations

$$\begin{aligned}\nabla \times \vec{E} &= -\partial_t \vec{B}, & \nabla \cdot \vec{B} &= 0, \\ \nabla \times \vec{H} &= \vec{j}_{\text{ex}} + \partial_t \vec{D}, & \nabla \cdot \vec{D} &= \rho_{\text{ex}}.\end{aligned}\tag{34}$$

The difference between \vec{H} and \vec{B} is supposed to come from spin of charge carriers, which comes from next order in \hbar , so we ignore. The electric displacement and electric field are related by $\vec{D} = \epsilon \vec{E}$, with ϵ being the dielectric constant characterizing the property of the medium. We may solve \vec{E} in momentum space as:

$$i \frac{\vec{q} \times (\vec{q} \times \vec{E})}{q_0} = \vec{j}_{\text{ex}} - i q_0 \epsilon \vec{E}.\tag{35}$$

(35) encodes response of \vec{E} to \vec{j}_{ex} . In the gauge $A_0 = 0$, (35) gives rise to the following retarded correlator

$$\begin{aligned}\langle A_i(q_0, \vec{q}) A_i(q'_0, \vec{q}') \rangle_R &\sim \frac{1}{q_0^2 \epsilon - q^2} \delta(q_0 + q'_0) \delta^3(\vec{q} + \vec{q}') \quad \vec{q} \perp \vec{A}, \\ \langle A_i(q_0, \vec{q}) A_i(q'_0, \vec{q}') \rangle_R &\sim \frac{1}{q_0^2 \epsilon} \delta(q_0 + q'_0) \delta^3(\vec{q} + \vec{q}') \quad \vec{q} \parallel \vec{A}.\end{aligned}\tag{36}$$

On the coarse-graining scale of the coordinate, the medium is known to be a very good conductor, so that we can parametrize the dielectric constant as

$$\epsilon \simeq 1 + \frac{i\sigma}{q_0},\tag{37}$$

with $\sigma \sim \frac{T}{\ell^2}$ [37,38]. For the purpose of parametric estimation, we will regard $q \sim q_0$ and not distinguish between longitudinal and transverse cases in (36). The retarded correlator in (36) dictates the symmetrized correlator of electromagnetic fields by fluctuation-dissipation

theorem [64]

$$\langle A_i(q_0, \vec{q}) A_i(q'_0, \vec{q}') \rangle_{sym} = \frac{2T}{q_0} \text{Im} \langle A_i(q_0, \vec{q}) A_i(q'_0, \vec{q}') \rangle_R \sim \frac{T}{q_0} \text{Im} \frac{1}{q_0^2 + i\sigma q_0} \delta(q_0 + q'_0) \delta^3(\vec{q} + \vec{q}'). \quad (38)$$

Noting that $\sigma \gg q_0$, we obtain the following estimate for fluctuation of electromagnetic gauge fields in coordinate space

$$|A_i(t, x)| \sim \left(\frac{q^3}{q_0 \sigma} \right)^{1/2} \sim e^5 T, \quad (39)$$

thus the effect of fluctuating electromagnetic fields can be ignored as long as the spacetime derivatives are much larger than the mean fluctuation of electromagnetic fields $\partial_X \gg e|A_i| \sim e^6 T$. The origin of the small fluctuation can be attributed to large conductivity, which disfavors fluctuation of electromagnetic fields.

vi. for the \hbar expansion to be valid, we require the quantum correction to be small. We shall obtain in Section 5 that $S^{<(1)} \sim \hbar \partial f$, which is to be compared with $S^{<(0)} \sim Pf$. This condition is clearly satisfied by $\partial_X \ll \Lambda$.

3 Elastic collisions

We begin with the $2 \rightarrow 2$ elastic collisions. These can be obtained from two-loop contributions to self-energies. As we shall see, there are both corrections to propagators and vertices. The former give squares of amplitude in separate channels, and the latter give interference terms between different channels.

In this section and the next one, we work solely with zeroth order quantities: $S^{</>(0)}$, $\Sigma^{</>(0)}$, $D_{\nu\rho}^{</>(0)}$, $\Pi^{\mu\nu </>(0)}$. To ease notations, we suppress the superscript (0).

3.1 propagator corrections

To be specific, we focus on the term $\Sigma^>(P)S^<(P)$. $\Sigma^>$ has the following representation

$$\Sigma^>(P) = e^2 \int_K \gamma^\mu S^>(K+P) \gamma^\nu D_{\nu\mu}^<(K). \quad (40)$$

Since P is on-shell, we cannot have both fermion momentum and photon momentum in the loop on-shell. Indeed, the one-loop contribution does not capture dissipation effects, for which two-loop diagrams are needed. The two-loop diagrams containing propagator corrections are shown in Fig. 1, in which the left/right diagrams has one fermion/photon

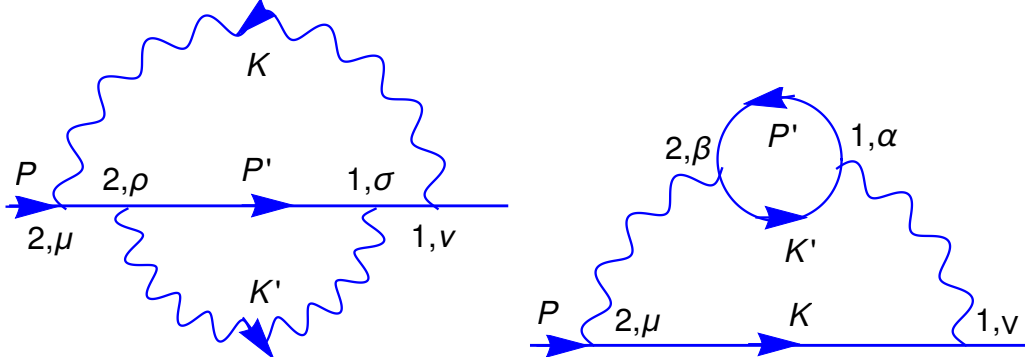


Figure 1: Two-loop diagrams for fermion self-energy containing propagator corrections. the 12 labeling are uniquely determined by the requirement that three propagators attached to a vertex cannot be simultaneously on-shell.

momentum off-shell. Note that the 12 labels are uniquely determined by the requirement that three propagators attached to a vertex cannot be simultaneously on-shell.

The left panel of Fig. 1 gives

$$\Sigma^>(P)S^<(P) = e^4 \int_{K,K'} \gamma^\mu S_{22}(K+P) \gamma^\rho S^>(P') \gamma^\sigma S_{11}(K+P) \gamma^\nu D_{\nu\mu}^<(K) D_{\rho\sigma}^>(K') S^<(P). \quad (41)$$

$\Sigma^<(P)S^>(P)$ can be obtained from (41) by the replacement $>\leftrightarrow<$ and $1 \leftrightarrow 2$. The dependences of $S^>/<(P)$ on f_e suggest that $\Sigma^>(P)S^<(P)$ and $\Sigma^<(P)S^>(P)$ correspond to loss and gain terms respectively. It is sufficient to focus on one of term only. We show in Appendix A that (41) give rise to squares of s-channel Compton scattering, u-channel Compton scattering and t-channel annihilation.

The right panel of Fig. 1 gives

$$\begin{aligned} \Sigma^>(P)S^<(P) &= -e^4 \int_{P',K'} \gamma^\mu S^>(K) \gamma^\nu D_{\mu\beta}^{22}(P-K) D_{\alpha\nu}^{11}(P-K) \text{tr}[\gamma^\alpha S^<(P') \gamma^\beta S^>(K')] \\ &\times S^<(P). \end{aligned} \quad (42)$$

Again the replacement $>\leftrightarrow<$ and $1 \leftrightarrow 2$ in the above leads to $\Sigma^<(P)S^>(P)$. We show in Appendix A that (42) give rise to squares of t-channel Coulomb scattering (between fermions), s-channel Coulomb scattering (between fermion and anti-fermion) and t-channel Coulomb scattering (between fermion and anti-fermion).

Next we turn to $\Pi^{\mu\nu>}(P)D_{\nu\mu}^<(P) - \Pi^{\mu\nu<}(P)D_{\nu\mu}^>(P)$. We focus on the term $\Pi^{\mu\nu>}(P)D_{\nu\rho}^<(P)$. Similar to the fermionic case, we look at two-loop photon self-energy diagrams containing propagator corrections. There is only one such diagram shown in Fig. 2. It gives the

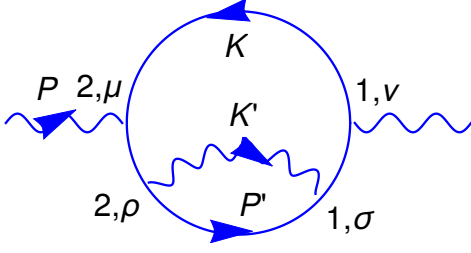


Figure 2: Two-loop diagrams for photon self-energy containing propagator corrections. the 12 labels are uniquely determined by the requirement that three propagators attached to a vertex cannot be simultaneously on-shell.

following contribution

$$\begin{aligned} \Pi^{\mu\nu>}(P)D_{\nu\mu}^<(P) &= -e^4 \int_{K,K'} \text{tr}[\gamma^\nu S^<(K)\gamma^\mu S^{22}(K+P)\gamma^\rho S^>(P')S^{11}(K+P)] \\ &\times D_{\rho\sigma}^>(K')D_{\nu\mu}^<(P). \end{aligned} \quad (43)$$

and a counterpart from $>\leftrightarrow<$ and $1\leftrightarrow 2$ of the above. We show in Appendix A that (43) give rise to squares of s-channel Compton scattering, u-channel Compton scattering and t-channel annihilation.

To compare with the spin-averaged Boltzmann equations by AMY [36–38], we note that square of u-channel annihilation and u-channel Coulomb (between fermions) are not present in our analysis. In fact, upon integration over phase space, they give identical contributions as their t-channel counterparts. The extra contributions in Boltzmann equations are precisely taken care of by the symmetry factor $\frac{1}{2}$ for identical particles in final states applicable for annihilation and Coulomb between fermions. Therefore we find agreement on the square of amplitudes in all channels for the collision term.

3.2 vertex corrections

The propagator corrections give square of amplitudes only. The interference between amplitudes arise from vertex corrections, which we discuss in the following. We begin with the simpler case of vertex correction in photon self-energy. In this case, only one diagram contributes, shown in Fig.3. Its contribution to collision term can be written as

$$\begin{aligned} \Pi^{\mu\nu>}(P)D_{\nu\mu}^<(P) &= -e^4 \int_{K,K'} \text{tr}[\gamma^\mu S^>(K)\gamma^\sigma S_{11}(K+K')\gamma^\nu S^<(P')\gamma^\rho S_{22}(K-P)] \\ &\times D_{\rho\sigma}^>(K')D_{\nu\mu}^<(P), \end{aligned} \quad (44)$$

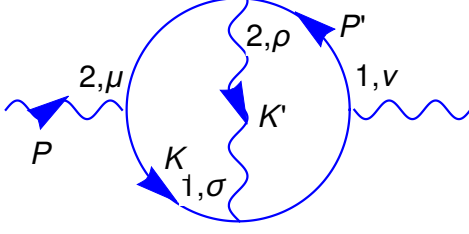


Figure 3: Two-loop diagrams for photon self-energy containing vertex corrections.

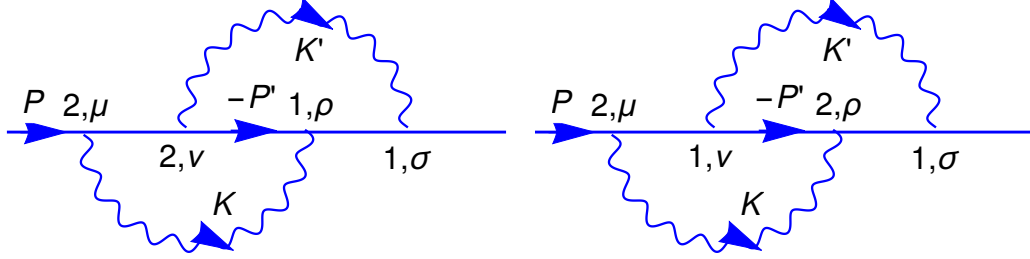


Figure 4: Two-loop diagrams for fermion self-energy containing vertex correction. There are two possible labelings of 12.

and $\Pi^{\mu\nu<}(P)D_{\nu\mu}^>(P)$ obtainable from the above by $>\leftrightarrow<$ and $1 \leftrightarrow 2$. In Appendix A, we show this give rise to *half of* interference terms of s/u-channels of Compton scattering and interference term of t/u-channels of annihilation.

Now we move to the vertex correction in fermion self-energy. We have two labelings for the vertex correction diagram shown in Fig.4. For the labeling on the left, we have the following contribution to collision term

$$\Sigma^>(P)S^<(P) = \int_{K,K'} \gamma^\mu S_{22}(P-K)\gamma^\nu S^>(-P')\gamma^\rho S_{11}(P-K')\gamma^\sigma D_{\nu\sigma}^>(K')D_{\mu\rho}^>(K)S^<(P). \quad (45)$$

We show in Appendix A that it gives rise to the following interference terms: *half of* t/u-channel for annihilation, s/t channel for Compton scattering.

For the other labeling on the right of Fig.4, we have the following contribution to collision term

$$\Sigma^>(P)S^<(P) = \int_{K,K'} \gamma^\mu S^>(P-K)\gamma^\nu S^<(-P')\gamma^\rho S^>(P-K')\gamma^\sigma D_{\mu\rho}^{22}(K)D_{\nu\sigma}^{11}(K')S^<(P). \quad (46)$$

It leads to the following interference terms: *half of* t/u-channels for Coulomb scattering (between fermions) and s/t-channels for Coulomb scattering (between fermion and anti-fermion).

Note that we have only half of the interference terms for annihilation and Coulomb scattering (between fermions). In fact in these cases, two interference terms are both real. Therefore, they again agree with the counterpart in Boltzmann equation when the symmetry factor $\frac{1}{2}$ for annihilation and Coulomb scattering (between fermions) is taken into account.

Finally we work out the effect of trace and contraction on the LHS of (32). Taking $p_0 > 0$, we have

$$\begin{aligned} 4P \cdot \partial \delta(P^2 - m^2) f_e(X, P) &= \frac{2}{E_p} P \cdot \partial f_e(X, P) \delta(p_0 - E_p), \\ 4P \cdot \partial \delta(P^2) f_\gamma(X, P) &= \frac{2}{p} P \cdot \partial f_\gamma(X, P) \delta(p_0 - p), \end{aligned} \quad (47)$$

with $E_p = (p^2 + m^2)^{1/2}$. Dividing out the prefactor 2 converts the spin-summed collision term to the spin-averaged one for either fermion or photon. We have only kept the particle contributions in (47). The kinetic equation for anti-particles can be obtained from the corresponding equations for $S^{<(0)}(X, -P)$ and $D_{\nu\rho}^{<(0)}(X, -P)$. Note that photon is its own anti-particle, so the resulting equation is expected to be equivalent. For fermions, we obtain for $p_0 > 0$

$$-4P \cdot \partial \delta(P^2 - m^2) f_e(X, -P) = \frac{2}{E_p} P \cdot \partial (1 - f_e(X, -P)) \delta(p_0 - E_p), \quad (48)$$

with $f_{\bar{e}}(X, P) \equiv 1 - f_e(X, -P)$ identified as distribution function for anti-fermions. Note that $f_e(X, P)$, $f_{\bar{e}}(X, P)$ and $f_\gamma(X, P)$ all have positive energies, so we may also denote them as $f_e(X, \vec{p})$, $f_{\bar{e}}(X, \vec{p})$ and $f_\gamma(X, \vec{p})$.

3.3 Screening effect

The elastic collisions occur either by exchanging off-shell photon (Coulomb scattering) or by exchanging off-shell fermion (Compton scattering and annihilation). Potential IR divergences exist when the exchange particles have soft momenta. It is known that the IR divergence can be rendered finite by the screening effect. Essentially the particles gain thermal mass by interaction with the off-equilibrium medium described by the kinetic theory, which effectively cuts off the divergence. The thermal mass scales as $e\Lambda$ for both fermion and photon with Λ being a characteristic scale of particle energies. When $m \gg e\Lambda$, the screening effect on Compton and annihilation is negligible: the bare mass of fermion plays the role of the cutoff. When $m \lesssim e\Lambda$, the screening effect is non-negligible. The case of Coulomb is special. Since photon is strictly massless, the screening effect provides the only

cutoff⁴. We will discuss two representative scenarios: $m \gg e\Lambda$ and $m \lesssim e\Lambda$. For the former, we only need thermal mass of photon. For the latter, we need thermal mass for both fermion and photon. All the quantities studied in this subsection are local in X , below we suppress the dependence on X for simplicity.

Now we work out the medium dependent thermal mass. We begin with the fermionic case. In elastic collisions, the exchanged off-shell fermions propagators S_{11}/S_{22} can be effectively replaced by S_R/S_A by using

$$S_{22}(P) = iS_A(P) + S^{\langle} (P), \quad S_{11}(P) = -iS_R(P) + S^{\langle} (P), \quad (49)$$

and the on-shell condition enforced by S^{\langle}/\rangle . Note that to $O(\hbar^0)$, the retarded and advanced propagators are related by “hermitian conjugate” for fermions and complex conjugate for photons:

$$S_A(P) = \gamma^0 S_R(P)^\dagger \gamma^0, \quad D_{\mu\nu}^A(P) = D_{\nu\mu}^{R*}(P). \quad (50)$$

So it is sufficient to consider medium modification to retarded propagators only. Let us consider the fermionic retarded self-energy, which satisfies the following equation

$$i\cancel{\partial}_x S_R(x, y) - m S_R(x, y) = -\delta(x - y) + \int d^4 z \Sigma_R(x, z) S_R(z, y), \quad (51)$$

which can be derived by taking both x and y in the upper branch in (4), and subtracting the resulting equation from (7). The Wigner transform of (51) to lowest order in \hbar satisfies

$$(\not{Q} - m - \Sigma_R(Q)) S_R(Q) = -1, \quad (52)$$

from which we can solve for the resummed propagator

$$S_R(Q) = -(\not{Q} - m - \Sigma_R(Q))^{-1}. \quad (53)$$

Σ_R is evaluated in Appendix B. We quote the result here

$$\Sigma_R(Q) = e^2 \int \frac{d^3 p}{(2\pi)^3} \frac{1}{2p} \frac{\cancel{P}}{P \cdot Q} (2f_\gamma(\vec{p}) + f_e(\vec{p}) + f_{\bar{e}}(\vec{p})). \quad (54)$$

Note that this result assumes $m \lesssim e\Lambda$ and we have dropped correction to $\Sigma_R(Q)$ of order $e^3 \Lambda^2/Q$ from including fermion mass in the loop. This is justified because the correction is maximized at $Q \sim e\Lambda$, for which $Q \sim m \gg e^3 \Lambda^2/Q$ so that the correction can be neglected in (52).

⁴In fact, the screening alone is not sufficient to cut off the divergence in Coulomb. A cancellation between loss and gain terms is needed to render the corresponding collision term finite.

The photonic case is in parallel. The retarded propagator in Coulomb gauge satisfies

$$\left(-Q^2 g^{\mu\nu} + Q^\mu Q^\nu - \frac{1}{\xi} P^{\mu\alpha} P^{\nu\beta} Q_\alpha Q_\beta\right) D_{\nu\rho}^R(Q) - \Pi_R^{\mu\nu} D_{\nu\rho}^R(Q) = -\delta_\rho^\mu. \quad (55)$$

This can be solved by

$$D_{\mu\nu}^R(Q) = \frac{-1}{Q^2 - \Pi_T^R} P_{\mu\nu}^T + \frac{-1}{q^2 + \Pi_L^R} u_\mu u_\nu + \xi \frac{Q_\mu Q_\nu}{q^4}, \quad (56)$$

where Π_T^R and Π_L^R are transverse and longitudinal components of retarded photon self-energy defined as

$$\Pi_{\mu\nu}^R = P_{\mu\nu}^T \Pi_T^R - \frac{Q^2}{q^2} P_{\mu\nu}^L \Pi_L^R. \quad (57)$$

We have introduced the longitudinal projector $P_{\mu\nu}^L = -g_{\mu\nu} + \frac{Q_\mu Q_\nu}{Q^2} - P_{\mu\nu}^T$ and $q^2 = -Q^2 + (Q \cdot u)^2$. We again set $\xi = 0$ for Coulomb gauge. $\Pi_{\mu\nu}^R$ is evaluated in Appendix B. We quote the result here

$$\Pi_{\mu\nu}^R = 2e^2 \int \frac{d^3p}{(2\pi)^3} \frac{1}{E_p} (f_e(\vec{p}) + f_{\bar{e}}(\vec{p})) (P_\mu Q_\nu + P_\nu Q_\mu - g_{\mu\nu} P \cdot Q) \frac{1}{P \cdot Q}, \quad (58)$$

which is applicable for both scenarios with mass dependence implicit in $E_p = \sqrt{p^2 + m^2}$.

For later use, we determine the thermal mass for hard on-shell fermions and transverse photons. (52) determines the fermion dispersion relation by:

$$Q - m - \Sigma_R(Q) = 0. \quad (59)$$

Following [72], we decompose the self-energy as $\Sigma_R = \Sigma_\mu^R \gamma^\mu + \Sigma_m^R 1$, which allows us to convert the matrix equation (59) into a scalar equation

$$(Q_\mu - \Sigma_\mu^R)^2 - (\Sigma_m^R + m)^2 = 0. \quad (60)$$

From (54), we have $\Sigma_\mu^R \sim e^2 \Lambda$ and $\Sigma_m^R = 0$. The thermal mass is identified as

$$\delta m_e^2 = 2Q^\mu \Sigma_\mu^R = e^2 \int \frac{d^3p}{(2\pi)^3} \frac{2}{p} (2f_\gamma(\vec{p}) + f_e(\vec{p}) + f_{\bar{e}}(\vec{p})). \quad (61)$$

The only change from the resummed propagator in equilibrium is that the thermal mass depends on the off-equilibrium distributions for fermion and photon. The photon thermal mass is determined from the pole of the transverse component of propagator as:

$$m_\gamma^2 = \Pi_T^R = \frac{1}{2} P_{\mu\nu}^T \Pi_R^{\mu\nu}. \quad (62)$$

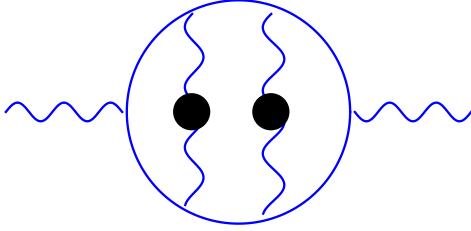


Figure 5: Photon self-energy containing vertex corrections from multiple scatterings. Arbitrary number of soft photon exchanges is possible. For illustration purpose we show two photon exchanges. The black dots indicate resummed photon propagators.

The contraction eliminates the terms proportional to $P_\mu Q_\nu + P_\nu Q_\mu$ in (58), leaving the following Q -independent expression

$$m_\gamma^2 = e^2 \int \frac{d^3p}{(2\pi)^3} \frac{2}{E_p} (f_e(\vec{p}) + f_{\bar{e}}(\vec{p})). \quad (63)$$

Summarizing this section, by considering propagator and vertex corrections, we have captured the full $2 \rightarrow 2$ elastic collision including screening effect in Boltzmann equation for QED.

4 Inelastic collisions

In the analysis of elastic scattering, we have excluded one-loop contribution to self-energies, which requires all three particles to be exactly collinear, leaving vanishing phase space. In fact, there is one exception: when we take into account thermal mass and damping of on-shell degree of freedoms, the energy conservation can be slightly violated, opening up a small phase space. It is known that in equilibrium both the thermal mass and damping rate give corrections to energy, which scale as $e^2\Lambda$. This allows for deviation of collinearity with transverse momenta scale as $e\Lambda$, giving rise to a phase space $e^2\Lambda^3$. Combining this with coupling constants in one-loop diagram, we have overall e^4 , which has the same powers of coupling constant as the two-loop diagrams. Furthermore, by pinching mechanism, fermions can have multiple soft scatterings with the medium, which all contribute at the same order and need to be added up coherently, known as Landau-Pomeranchuk-Migdal effect. The multiple scatterings are encoded in another type of vertex corrections in self-energies diagrams, shown in Fig. 5. It involves multiple insertions of soft photon propagators.

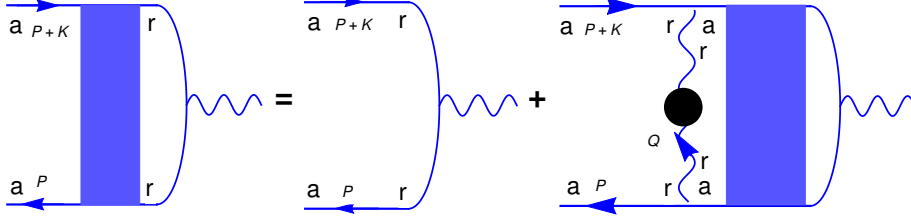


Figure 6: Diagrammatic equation satisfied by the resummed vertex. We will consider spin-dependent vertex, in which the fermions with momenta $P + K$ and P carrying spin labels s and t .

4.1 Resummed vertex

Let us illustrate the pinching mechanism by looking at the resummed vertex. Following [73], the evaluation is most conveniently done in the ra basis, in which only one inequivalent labeling is allowed⁵. The resummed vertex satisfies the diagrammatic equation in Fig. 6. The pinching mechanism can be seen by inspecting the energy integration of two side-rails

$$\int \frac{dp_0}{2\pi} S_{ra}(P)(\dots)S_{ar}(K+P), \quad (64)$$

with $S_{ra} = D_{ra}(P)(\not{P} + m)$ and $S_{ar} = D_{ar}(K+P)(\not{K} + \not{P} + m)$. D_{ra} and D_{ar} are the same as scalar propagators given by⁶

$$\begin{aligned} D_{ra}(P) &= \frac{i}{(p_0 + \frac{i}{2}\Gamma_p)^2 - E_p^2}, \\ D_{ar}(K+P) &= \frac{i}{(p_0 + k_0 - \frac{i}{2}\Gamma_{p+k})^2 - E_{p+k}^2}. \end{aligned} \quad (65)$$

To be specific, we take $k_0 > 0$, Let us evaluate the following by residue theorem

$$\int \frac{dp_0}{2\pi} D_{ra}(P)D_{ar}(K+P). \quad (66)$$

The poles are located at $p_0 = \pm E_p - \frac{i}{2}\Gamma_p$, $p_0 = -k_0 \pm E_{p+k} + \frac{i}{2}\Gamma_{p+k}$. Here P is allowed to have transverse component $p_\perp \sim e\Lambda$. With the deviation from collinearity and the thermal/bare mass, we have

$$\begin{aligned} E_p &= p + \frac{p_\perp^2 + \delta m_e^2 + m^2}{2p}, \\ E_{p+k} &= |\mathbf{p} + \mathbf{k}| + \frac{p_\perp^2 + \delta m_e^2 + m^2}{2|\mathbf{p} + \mathbf{k}|}, \\ k_0 &= k + \frac{m_\gamma^2}{2k}, \end{aligned} \quad (67)$$

⁵The other one is related by interchanging r and a . All other labelings can be related to the two.

⁶ $\frac{\Gamma}{2}$ is defined as the damping rate here.

Denoting $p_{\parallel} = \vec{p} \cdot \hat{k}$, we can rewrite the poles as $p_0 = \pm p_{\parallel} - \frac{i}{2}\Gamma_p$, $p_0 = -k_0 \pm (p_{\parallel} + k) + \frac{i}{2}\Gamma_{p+k}$. The pinching mechanism is at work when two of the poles nearly pinch. Ignoring the thermal masses and damping rate, we find the poles at $p_0 = p_{\parallel}$ and $p_0 = -k_0 + p_{\parallel} + k$ coincide. The thermal masses and damping rates provides necessary regularization to the divergence. Closing the contour and picking up one of the pinching poles, we obtain

$$\int \frac{dp_0}{2\pi} D_{ra}(P) D_{ar}(K+P) = \frac{-1}{4p_{\parallel}(p_{\parallel} + k)(i\delta E + \Gamma)}, \quad (68)$$

with

$$\begin{aligned} \delta E &= k_0 + E_p \epsilon(p_{\parallel}) - E_{p+k} \epsilon(p_{\parallel} + k) \simeq \frac{k(p_{\perp}^2 + \delta m_e^2 + m^2)}{2p_{\parallel}(p_{\parallel} + k)} + \frac{m_{\gamma}^2}{2k}, \\ \Gamma &= \frac{1}{2} (\Gamma_p + \Gamma_{p+k}). \end{aligned} \quad (69)$$

In the scenario $m \lesssim e\Lambda$, $\delta E \sim e^2\Lambda$ and Γ is evaluated in appendix C to be at the same order. Thus we have an enhancement factor e^{-2} from the pinching mechanism. For each insertion of a pair of pinching propagators (side-rails) and soft photon propagator (rung) in Fig. 6, we have the following power counting: pinch enhancement factor e^{-2} , e^2 from the coupling constants, e^3 from the phase space of soft photon and e^{-3} from its propagator⁷, which leads to an overall factor e^0 , thus arbitrary number of insertions are allowed, corresponding to multiple soft scatterings of hard fermions with the medium fermions. However in the scenario $m \gg e\Lambda$, the pinching mechanism is suppressed. It follows that inelastic scattering is irrelevant in this scenario to the order of our interest. Below we proceed with the scenario $m \lesssim e\Lambda$.

We denote the resummed vertex in Fig. 6 as $\Gamma_{st}^{\mu}(P+K, P)$, with s, t labeling the spinors in the outermost propagators carrying momenta $P+K$ and P respectively. This is a polarization-dependent vertex between two on-shell fermions with spin s, t and one on-shell photon. We can take the Lorentz index μ to be transverse, since the resulting self-energy will be contracted with projector in (33). Below we denote μ by M for transverse indices. Below we first consider the case $p_0 > 0$, for which Γ_{st}^M can be interpreted as the amplitude of a fermion (with momentum $P+K$ and spin s) splitting into a fermion (with momentum P and spin t) and a photon (with momentum K and polarization ε^M). We can

⁷an additional e^{-1} is from Bose enhancement factor

express the diagrammatic equation as⁸

$$\begin{aligned} \Gamma_{st}^M(P+K, P) &= D_{ra}(P)D_{ar}(P+K)u_s(P+K)\bar{u}_s(P+K)\gamma^M u_t(P)\bar{u}_t(P) \\ &+ \int_Q D_{ra}(P)D_{ar}(P+K) ((\not{P} + \not{K})(-ie\gamma^\mu)\Gamma_{st}^M(P+K+Q, P+Q)(-ie\gamma^\nu)\not{P}) D_{\nu\mu}^{rr}(Q), \end{aligned} \quad (70)$$

where the structures $u_s(P+K)\bar{u}_s(P+K)$ and $u_t(P)\bar{u}_t(P)$ come from $\not{P} + \not{K}$ and \not{P} projected onto given spin states respectively. Note that we have dropped the subleading masses in the numerators of fermion propagators. We will use the following representation for spinors

$$u_s(P) = \sqrt{\frac{p_0}{2}} \begin{pmatrix} (1 - \sigma \cdot \vec{p}/p_0)\xi_s \\ (1 + \sigma \cdot \vec{p}/p_0)\xi_s \end{pmatrix}, \quad (71)$$

with $\xi_+ = (1, 0)^T$ and $\xi_- = (0, 1)^T$. In this representation, the spin label $s = \pm$ corresponds to spin being parallel/anti-parallel to momentum. We can derive the following relations valid to leading order in e

$$\begin{aligned} \bar{u}_s(P+K)\gamma^\mu u_{s'}(P+Q+K) &\simeq \delta_{ss'} 2(P+K)^\mu, \\ \bar{u}_{t'}(P+Q)\gamma^\nu u_t(P) &\simeq \delta_{tt'} 2P^\nu, \\ \bar{u}_s(P+K)\gamma^M u_t(P) &\simeq (p_\parallel(p_\parallel+k))^{-1/2} \left((p_\parallel+k)p_\parallel^M + p_\parallel p_{-s}^M \right) \delta_{st}, \end{aligned} \quad (72)$$

with $p_\pm^M = p^M \pm i\epsilon^{MN}p^N$ and we have used the pinching condition $p_0 \simeq p_\parallel$. We easily deduce the spin direction of the fermion along the upper/lower rails is not changed. We can parametrize the vertex by

$$\Gamma_{st}^M(P+K, P) = \delta_{st} u_s(P+K)\bar{u}_t(P) (p_\parallel(p_\parallel+k))^{-1/2} \left((p_\parallel+k)p_s^M + p_\parallel p_{-s}^M \right) \Gamma_s(P). \quad (73)$$

By rotational invariance, $\Gamma(P)$ is a function of p_\parallel, p_\perp^2 . It follows then

$$\begin{aligned} ((p_\parallel+k)p_s^M + p_\parallel p_{-s}^M) \Gamma_s(P) &= ((p_\parallel+k)p_s^M + p_\parallel p_{-s}^M) D_{ra}(P)D_{ar}(P+K) \\ &- e^2 \int_Q D_{ra}(P)D_{ar}(P+K) ((p_\parallel+k)(p+q)_s^M + p_\parallel(p+q)_{-s}^M) \Gamma_s(P+Q) 4p_\parallel(p_\parallel+k) \\ &\times \hat{K}^\mu \hat{K}^\nu D_{\nu\mu}^{rr}(Q). \end{aligned} \quad (74)$$

By pinching mechanism, the vertex should have support localized on the pole $p_0 = p_\parallel$. The same kinematic restriction should apply to the bare vertex in the diagrammatic equation in Fig. 6. It is then convenient to define

$$\int \frac{dp_0}{2\pi} \Gamma_s(P) = -\frac{1}{4p_\parallel(p_\parallel+k)} \chi_s(P). \quad (75)$$

⁸An overall $-ie$ is factored out from the vertex.

In terms of χ_s , (74) becomes

$$\begin{aligned} & - ((p_{\parallel} + k)p_s^M + p_{\parallel}p_{-s}^M) \chi_s(P)(i\delta E + \Gamma) = - ((p_{\parallel} + k)p_s^M + p_{\parallel}p_{-s}^M) \\ & - e^2 \int \frac{d^3q}{(2\pi)^3} ((p_{\parallel} + k)(p + q)_s^M + p_{\parallel}(p + q)_{-s}^M) \chi_s(P + Q) \hat{K}^{\mu} \hat{K}^{\nu} D_{\nu\mu}^{rr}(Q). \end{aligned} \quad (76)$$

(76) can be further simplified by using the following representation of Γ :

$$\Gamma = e^2 \int \frac{d^3q}{(2\pi)^3} \hat{K}^{\mu} \hat{K}^{\nu} D_{\nu\mu}^{rr}(Q). \quad (77)$$

It contains the same soft photon propagator as in (76). A derivation of the representation can be found in Appendix C. Using (77), we can rewrite (76) as

$$\begin{aligned} & ((p_{\parallel} + k)p_s^M + p_{\parallel}p_{-s}^M) = ((p_{\parallel} + k)p_s^M + p_{\parallel}p_{-s}^M) \chi_s(P) i\delta E + e^2 \int \frac{d^3q}{(2\pi)^3} \hat{K}^{\mu} \hat{K}^{\nu} D_{\nu\mu}^{rr}(Q) \\ & [((p_{\parallel} + k)p_s^M + p_{\parallel}p_{-s}^M) \chi_s(P + Q) - ((p_{\parallel} + k)(p + q)_s^M + p_{\parallel}(p + q)_{-s}^M) \chi_s(P + Q)]. \end{aligned} \quad (78)$$

The structure $(p_{\parallel} + k)p_s^M + p_{\parallel}p_{-s}^M$ encodes the spin dependence of the vertex. It is more transparent to switch to circular polarizations for the photon $\varepsilon_{\pm}^M = \frac{1}{\sqrt{2}}(0, 1, \pm i, 0)$. The corresponding coordinates and momenta are defined by $x^{\pm} = \frac{1}{\sqrt{2}}(x \pm iy)$ and $p^{\pm} = \frac{1}{\sqrt{2}}(p_x \pm ip_y)$, with $M = \pm$ in the circular basis. Using $p_+^M = (\sqrt{2}p^+, 0)$, $p_-^M = (0, \sqrt{2}p^-)$, we find (78) splits into two cases $s = \pm M$, which satisfy a unified equation

$$p^M = p^M \chi_s(P) i\delta E + e^2 \int \frac{d^3q}{(2\pi)^3} \hat{K}^{\mu} \hat{K}^{\nu} D_{\nu\mu}^{rr}(Q) [p^M \chi_s(P + Q) - (p + q)^M \chi_s(P + Q)]. \quad (79)$$

Recall in our \hbar expansion, f_e is spin independent. It follows from (130) and (132) that the kernel $\hat{K}^{\mu} \hat{K}^{\nu} D_{\nu\mu}^{rr}(Q)$ is also spin independent. A spin independent $\chi_s = \chi$ is expected from (79). Furthermore, (79) is manifestly rotational invariant, which is equally valid in the orthogonal basis. (79) in the orthogonal basis is in agreement with Eqs.(2.2) and (2.6) of [36], with the identification $\chi = \frac{1}{2}\chi_{AMY}$.

Although spin information is averaged out in the resulting kinetic theory, the spin dependence of the vertex is instructive on its own. The structure $(p_{\parallel} + k)p_s^M + p_{\parallel}p_{-s}^M$ in circular basis indicates that a fermion with spin in either direction can radiate a right/left handed photon without changing its spin. Clearly spin angular momentum is not conserved. Since collision is local, orbital angular momentum is zero before and after the collision. The change of spin angular momentum comes from spin exchange between the fermion/photon in the resummed vertex and fermions in the medium, whose spin information is averaged out.

4.2 photon self-energy

From Fig. 6, the resummed vertex Γ_{st}^M contains the four-fermi correlators $G_{aarr}(P+K, P, P+K+Q, P+Q)$ with $P+K$ and P labeled by a and $P+K+Q$ and $P+Q$ labeled by r as in Fig. 6. In the pinching kinematical region, $Q \ll P \& K$. To convert to photon self-energy, we need $G_{1122}(P+K, P, P+K+Q, P+Q)$. The conversion involves an off-equilibrium generalization of Kubo-Martin-Schwinger (KMS) relation. We give a diagrammatic derivation of the relation in the pinching kinematical region in Appendix D. The off-equilibrium relation simply replaces the equilibrium distribution by the off-equilibrium counterpart as

$$G_{1122}(P+K, P, P+K+Q, P+Q) = f_e(p_{\parallel} + k)(1 - f_e(p_{\parallel}))2\text{Re}G_{aarr}(P+K, P, P+K+Q, P+Q). \quad (80)$$

Accordingly, to obtain the photon self-energy $\Pi^{\langle}(K) = \int_{P,Q} G_{1122}(P+K, P, P+K+Q, P+Q)$, we should use $f_e(p_{\parallel} + k)(1 - f_e(p_{\parallel}))2\text{Re}[\Gamma_{st}^M]$ as the correct resummed vertex. Now we can trace $-ie\Gamma_{st}^M(P+K, P)$ with $-ie\gamma^N$, include -1 from fermion loop, sum over spins and integrate over momentum to obtain

$$\begin{aligned} \Pi^{\langle MN}(K) &= \int_P (-1)(-ie)^2 \sum_{s,t} \text{tr}[\Gamma_{st}^M(P+K, P)\gamma^N] \\ &= e^2 \sum_s \int \frac{d^3p}{(2\pi)^3} \frac{1}{4(p_{\parallel}(p_{\parallel} + k))^{3/2}} ((p_{\parallel} + k)p_s^M + p_{\parallel}p_{-s}^M) f_e(p_{\parallel} + k)(1 - f_e(p_{\parallel})) \\ &\quad \times 2\text{Re}[\chi(P)]\text{tr}[u_s(P+K)\bar{u}_s(P)\gamma^N]. \end{aligned} \quad (81)$$

Recall in (33), $\Pi^{\langle MN}$ is contracted with $D_{MN}^{\rangle}(K) \propto P_{MN}^T f_{\gamma}(k)$. We can use the following for the trace

$$\text{tr}[u_s(P+K)\bar{u}_s(P)\gamma^N] = (p_{\parallel}(p_{\parallel} + k))^{-1/2} ((p_{\parallel} + k)p_{-s}^N + p_{\parallel}p_s^N). \quad (82)$$

By the s -independent identity

$$\sum_M p_s^M p_{-s}^M = 2p_{\perp}^2, \quad \sum_M p_s^M p_s^M + p_{-s}^M p_{-s}^M = 0, \quad (83)$$

we can see the spin sum simply gives a factor of 2. In the end, we arrive at

$$\Pi^{\langle MN} D_{MN}^{\rangle} = e^2 \int \frac{d^3p}{(2\pi)^3} f_e(p_{\parallel} + k)(1 - f_e(p_{\parallel}))(1 + f_{\gamma}(k))2\text{Re}[\chi(P)] \frac{((p_{\parallel} + k)^2 + p_{\parallel}^2) p_{\perp}^2}{(p_{\parallel}(p_{\parallel} + k))^2}. \quad (84)$$

The other collision term $\Pi^{\rangle MN} D_{MN}^{\langle}$ is obtainable from (84) by the replacement of the distribution functions $f_e(p_{\parallel} + k)(1 - f_e(p_{\parallel}))(1 + f_{\gamma}(k)) \rightarrow (1 - f_e(p_{\parallel} + k))f_e(p_{\parallel})f_{\gamma}(k)$.

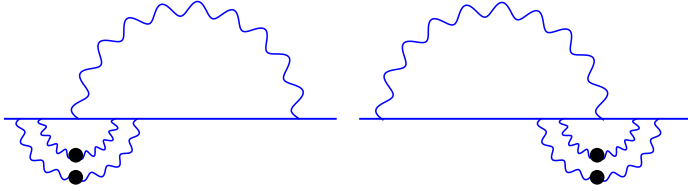


Figure 7: Fermion self-energy containing vertex corrections from multiple scatterings. Arbitrary number of soft photon exchanges is possible. Unlike the photonic case, there are two inequivalent vertex corrections.

So far, we have focused on the kinematical region with $p_0 > 0$ and $k_0 > 0$. Let us first lift $p_0 > 0$. Other possible kinematical regions are $p_0 + k < 0$ corresponding to anti-fermion bremsstrahlung and $-k < p_0 < 0$ corresponding to inelastic annihilation. For $p_0 + k < 0$, we use the following projections for spin states.

$$\begin{aligned} \not{P} + \not{K} &\rightarrow -u_s(-P - K)\bar{u}_s(-P - K), \\ \not{P} &\rightarrow -u_t(-P)\bar{u}_t(-P). \end{aligned} \quad (85)$$

The contraction of vertices is modified slightly from (72) as

$$\begin{aligned} \bar{u}_s(-P - K)\gamma^\mu u_{s'}(-P - Q - K) &\simeq -\delta_{ss'} 2(P + K)^\mu, \\ \bar{u}_{t'}(-P)\gamma^\nu u_t(-P - Q) &\simeq -\delta_{tt'} 2P^\nu, \\ \bar{u}_s(-P - K)\gamma^M u_t(-P) &\simeq (p_{\parallel}(p_{\parallel} + k))^{-1/2} \left((p_{\parallel} + k)p_{\parallel}^M + p_{\parallel}p_{-s}^M \right) \delta_{st}. \end{aligned} \quad (86)$$

With these, we easily confirm (84) is also applicable for $p_0 < -k$. The analysis for $-k < p_0 < 0$ is similar, with $p_{\parallel}(p_{\parallel} + k)$ replaced by $-p_{\parallel}(p_{\parallel} + k)$, which leaves (84) unchanged. This justifies extending the integration domain of p_{\parallel} to $(-\infty, \infty)$.

Finally we comment on the case $k_0 < 0$. This case would be needed for the dynamics of photon's anti-particle. Since photon's anti-particle is itself, we expect it to give an equivalent equation.

4.3 fermion self-energy

Unlike the photonic case, the fermion self-energy arises from two diagrams shown in Fig.7. To be specific, let us consider $p_0 > 0$ corresponding to fermion. We consider the term $\Sigma^>S^<(\Sigma^<S^>)$ and focus on the second diagram first. It is convenient to include the contribution $\Sigma_{22}S_{22}(\Sigma_{11}S_{11})$. Upon taking the trace, we have from the diagrammatic identity

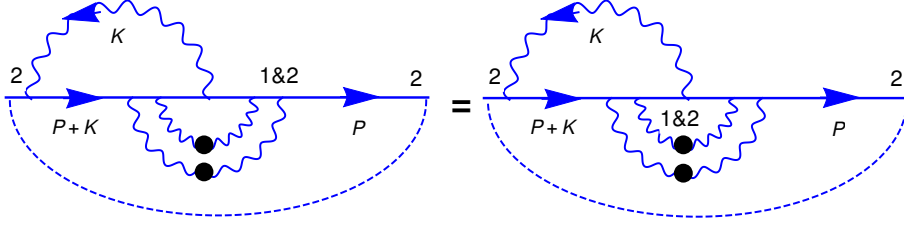


Figure 8: The LHS and RHS has one-to-one correspondence with the first line of (87). The symbol 1&2 indicates the vertex can be labeled by either 1 or 2, giving rise to two terms. The dashed line corresponds to the trace in the left diagram and the contraction in the right diagram. Replacing the outermost labels 2 by 1 leads to the second line of (87).

in Fig. 8 that

$$\begin{aligned}
\text{tr}[\Sigma^{\>}(P)S^{\<}(P) + \Sigma_{22}(P)S_{22}(P)] &= \int_K [G^{\mu\nu>}(P+K, P)D_{\nu\mu}^{\<}(K) + G_{22}^{\mu\nu}(P+K, P)D_{\nu\mu}^{22}(K)], \\
\text{tr}[\Sigma^{\<}(P)S^{\>}(P) + \Sigma_{11}(P)S_{11}(P)] &= \int_K [G^{\mu\nu<}(P+K, P)D_{\nu\mu}^{\<}(K) + G_{11}^{\mu\nu}(P+K, P)D_{\nu\mu}^{11}(K)],
\end{aligned} \tag{87}$$

where $G^{\mu\nu}(P+K, P)$ are partially-integrated photon self-energy defined as

$$\begin{aligned}
G^{\mu\nu>}(P+K, P) &= \int_Q \text{tr}[(-ie\gamma^\mu)G_{2211}(P+K, P, P+K+Q, P+Q)(-ie\gamma^\nu)], \\
G^{\mu\nu<}(P+K, P) &= \int_Q \text{tr}[(-ie\gamma^\mu)G_{1122}(P+K, P, P+K+Q, P+Q)(-ie\gamma^\nu)], \\
G_{22}^{\mu\nu}(P+K, P) &= \int_Q \text{tr}[(-ie\gamma^\mu)G_{2222}(P+K, P, P+K+Q, P+Q)(-ie\gamma^\nu)], \\
G_{11}^{\mu\nu}(P+K, P) &= \int_Q \text{tr}[(-ie\gamma^\mu)G_{1111}(P+K, P, P+K+Q, P+Q)(-ie\gamma^\nu)].
\end{aligned}$$

Taking the difference of the two lines in (87), we obtain (with arguments suppressed)

$$\begin{aligned}
&\text{tr}[\Sigma^{\>}S^{\<} - \Sigma^{\<}S^{\>} + \Sigma_{22}S_{22} - \Sigma_{11}S_{11}] \\
&= \int_K [G^{\mu\nu>}D_{\nu\mu}^{\>} - G^{\mu\nu<}D_{\nu\mu}^{\<} + G_{22}^{\mu\nu}D_{\nu\mu}^{22} - G_{11}^{\mu\nu}D_{\nu\mu}^{11}].
\end{aligned} \tag{88}$$

Using that $\Sigma^{\>/\<}$ and $S^{\>/\<}$ are ‘‘hermitian’’, we can easily show $\text{tr}[\Sigma^{\>}S^{\<} - \Sigma^{\<}S^{\>}]$ is real.

Further using the following hermitian properties

$$\begin{aligned}
\Sigma_{22} &= \gamma^0 \Sigma_{11}^\dagger \gamma^0, & S_{22} &= \gamma^0 S_{11}^\dagger \gamma^0, \\
G_{22}^{\mu\nu} &= G_{11}^{\nu\mu*}, & D_{22}^{\mu\nu} &= D_{11}^{\nu\mu*},
\end{aligned} \tag{89}$$

we obtain from (88)

$$\begin{aligned} & \text{tr}[\Sigma^>(P)S^<(P) - \Sigma^<(P)S^>(P)] = \text{Re}(\text{tr}[\Sigma^>(P)S^<(P) - \Sigma^<(P)S^>(P)]) \\ & = \int_K [G^{\mu\nu>}(P+K, P)D_{\nu\mu}^<(K) - G^{\mu\nu<}(P+K, P)D_{\nu\mu}^>(K)], \end{aligned} \quad (90)$$

The evaluation of the first diagram proceeds similarly. We have instead

$$\begin{aligned} & \text{tr}[\Sigma^>(P)S^<(P) - \Sigma^<(P)S^>(P)] \\ & = \int_K [G^{\mu\nu<}(P, P+K)D_{\nu\mu}^<(K) - G^{\mu\nu>}(P, P+K)D_{\nu\mu}^>(K)]. \end{aligned} \quad (91)$$

Note that the momenta argument in (90) and (91) differ. Using $G^{\mu\nu<}(P, P+K) = G^{\nu\mu>}(P+K, P)$ and the fact that $D_{\nu\mu}^{</>}$ is symmetric in $\mu\nu$, we easily see the two diagrams give identical contributions. One may wonder about the contribution when both vertices are resummed. We show by enumeration in Appendix E that such contribution is not allowed.

Note that $p_0 = p$ with our choice. It is useful to rearrange our results above. Using the reciprocal relations (21) and (31), we can deduce diagrammatically analogous relation holds for fermion self-energy from the pinching kinematical region.

$$\Sigma^>(P) = \overline{\Sigma}^<(-P) = \Sigma^<(-P). \quad (92)$$

In the second equality, we have removed the overline because we have dropped the subleading mass next to \not{P} and mass always appears in squares elsewhere. We can then rewrite

$$\begin{aligned} \text{tr}[\Sigma^>(P)S^<(P)]|_{2\text{nd}} &= \text{tr}[\Sigma^<(-P)S^>(-P)]|_{1\text{st}}, \\ \text{tr}[\Sigma^<(P)S^>(P)]|_{2\text{nd}} &= \text{tr}[\Sigma^>(-P)S^<(-P)]|_{1\text{st}}, \end{aligned} \quad (93)$$

where the subscripts 1st and 2nd denote contributions from the first and second diagrams in Fig.7 respectively. This allows us to reexpress the contributions in the region $p_0 = p$ from two diagrams to the counterpart in the region $p_0 = \pm p$ from a single diagram:

$$\begin{aligned} & \text{tr}[\Sigma^>(P)S^<(P) - \Sigma^<(P)S^>(P)]|_{1\text{st}+2\text{nd}} \\ & = \text{tr}[\Sigma^>(P)S^<(P) - \Sigma^<(P)S^>(P) - \Sigma^>(-P)S^<(-P) + \Sigma^<(-P)S^>(-P)]|_{1\text{st}} \end{aligned} \quad (94)$$

In fact, the RHS of (94) is closely related to (84). Note that $\Pi^{MN</>}(K) = \int_P G^{MN</>}(P+K, P)$. We would have the collision term of photon if the momentum integration is done over P instead of K . To establish the relation, we first integrate $G^{MN</>}$ over transverse components of momentum so that the resulting collision term has natural interpretation as collinear $1 \leftrightarrow 2$ processes. This can be conveniently done by converting d^2k_\perp to d^2p_\perp .

The key observation is that the geometrically invariant quantity here is the opening angle θ between \vec{p} and \vec{k} , which is bounded by the integrand as $\theta \lesssim \frac{m_\gamma}{p} \sim O(e)$. Using spherical coordinates, we can easily show

$$\int \frac{d^2 k_\perp}{(2\pi)^2} = \frac{k^2}{p^2} \int \frac{d^2 p_\perp}{(2\pi)^2}. \quad (95)$$

The remaining complication is in the integration of k_0 . On one hand, $G^{MN</>}$ contains $\delta(p_0 - p_\parallel \epsilon(k_0))$ according to the pinching mechanism. On the other hand $\delta(K^2)$ from $D_{MN}^{</>} = \frac{1}{2k} (\delta(k_0 - k) + \delta(k_0 + k))$ receives contribution from two poles. For $k_0 = k$, it gives the following contribution

$$\begin{aligned} \int_K G^{MN>} D_{MN}^{<} &= \int_0^\infty \frac{dk}{2\pi} \int \frac{d^2 p_\perp}{(2\pi)^2} \frac{k}{2p^2} f_e(p_\parallel) (1 - f_e(p_\parallel + k)) 2\text{Re}[\chi(P)] 2\pi \delta(p_0 - p_\parallel) \\ &\frac{\left((p_\parallel + k)^2 + p_\parallel^2 \right) p_\perp^2}{\left(p_\parallel (p_\parallel + k) \right)^2} 2\pi (1 + f_\gamma(K)). \end{aligned} \quad (96)$$

For $k_0 < -k$, we have instead

$$\begin{aligned} \int_K G^{MN>} D_{MN}^{<} &= \int_0^\infty \frac{dk}{2\pi} \int \frac{d^2 p_\perp}{(2\pi)^2} \frac{k}{2p^2} f_e(-p_\parallel) (1 - f_e(-p_\parallel - k)) 2\text{Re}[\chi(P)] 2\pi \delta(p_0 + p_\parallel) \\ &\frac{\left((-p_\parallel - k)^2 + p_\parallel^2 \right) p_\perp^2}{\left(-p_\parallel (-p_\parallel - k) \right)^2} 2\pi (1 + f_\gamma(K)). \end{aligned} \quad (97)$$

Note that we need to have $p_\parallel > 0$ ($p_\parallel < 0$) for $k_0 > 0$ ($k_0 < 0$) respectively in order to give the pole contribution at $p_0 = p$ for fermion. We can then combine (96) and (97) to write

$$\begin{aligned} \text{tr}[\Sigma^>(P)S^<(P) - \Sigma^<(P)S^>(P)] &= \int \frac{dk_\parallel}{2\pi} \int \frac{d^2 p_\perp}{(2\pi)^2} \frac{k}{2p^2} f_e(p) (1 - f_e(p + k_\parallel)) \\ &\times 2\text{Re}[\chi(P)] 2\pi \delta(p_0 - p) \frac{\left((p + k_\parallel)^2 + p^2 \right) p_\perp^2}{\left(p(p + k_\parallel) \right)^2} 2\pi (1 + f_\gamma(K)). \end{aligned} \quad (98)$$

(98) is in agreement with Eq.(2.7) of [36] when specialized to $U(1)$ gauge group.

5 Quantum correction to the solutions

With the solutions to the distributions f_e and f_γ from the classical kinetic equation, we can proceed to the quantum correction. We first consider the quantum correction to fermion Wigner function $S^{<(1)}$, which satisfies

$$\frac{i}{2} \not{\partial} S^{<(0)} + \frac{\not{P} - m}{\hbar} S^{<(1)} = \frac{i}{2} \left(\Sigma^{>(0)} S^{<(0)} - \Sigma^{<(0)} S^{>(0)} \right). \quad (99)$$

Recall that f_e is distributions for both left/right-handed component of fermions. It is known that for massless fermion, distribution is not frame independent. Side-jump needs to be taken into account in order to restore the frame independence of physical quantities [74, 75]. The side-jump manifests itself as an induced $O(\hbar)$ quantum correction to the Wigner function [22, 76]. Similar situation has been found for massive fermions [42, 77], where quantum correction for both axial and tensor components have been induced:

$$S^{<(1)}(P) = \gamma^5 \gamma_\mu \mathcal{A}^\mu + \frac{i[\gamma_\mu, \gamma_\nu]}{4} \mathcal{S}^{\mu\nu}, \quad (100)$$

where

$$\begin{aligned} \mathcal{A}^\mu &= -2\pi\hbar\epsilon(P \cdot u) \frac{\epsilon^{\mu\nu\rho\sigma} P_\rho u_\sigma \mathcal{D}_\nu f_e}{2(P \cdot u + m)} \delta(P^2 - m^2), \\ \mathcal{S}^{\mu\nu} &= -2\pi\hbar\epsilon(P \cdot u) \frac{\mathcal{D}_{[\mu} P_{\nu]} f_e - m u_{[\mu} \mathcal{D}_{\nu]} f_e - P_{[\mu} u_{\nu]} \mathcal{D}_m}{2(P \cdot u + m)} \delta(P^2 - m^2). \end{aligned} \quad (101)$$

The collisional effect is taken into account in the definitions $\mathcal{D}_\nu = \partial_\nu - \Sigma_\nu^> - \Sigma_\nu^<$ with $\frac{1-f_e}{f_e}$ and $\mathcal{D}_m = \Sigma_m^> + \Sigma_m^<$ with $\frac{1-f_e}{f_e}$ with $\Sigma_\nu^>/< = \frac{1}{4}\text{tr}[\Sigma^>/<\gamma_\nu]$ and $\Sigma_m^>/< = \frac{1}{4}\text{tr}[\Sigma^>/<]$.

The quantum correction to photon Wigner function $D_{\nu\rho}^{<(1)}$ satisfies the following equation up to $O(\hbar)$

$$\begin{aligned} &\left(-P^2 g^{\mu\nu} + P^\mu P^\nu - \frac{1}{\xi} P^{\mu\alpha} P^{\nu\beta} P_\alpha P_\beta\right) D_{\nu\rho}^{<(1)} + \frac{i}{2} \left(-2P \cdot \partial g^{\mu\nu} + \partial^\mu P^\nu + \partial^\nu P^\mu\right. \\ &\left. - \frac{1}{\xi} P^{\mu\alpha} P^{\nu\beta} (\partial_\alpha P_\beta + \partial_\beta P_\alpha)\right) D_{\nu\rho}^{<(0)} = \frac{i}{2} \left(\Pi^{\mu\nu>(0)} D_{\nu\rho}^{<(0)} - \Pi^{\mu\nu<(0)} D_{\nu\rho}^{>(0)}\right), \end{aligned} \quad (102)$$

With the help of the gauge fixing term, we can solve (102) by the following inversion

$$\left(\frac{u_\mu u_\lambda}{\mathbf{p}^2} + \frac{P_{\mu\lambda}^T}{P^2} - \xi \frac{P_\mu P_\lambda}{\mathbf{p}^4}\right) \left(-P^2 g^{\mu\nu} + P^\mu P^\nu - \frac{1}{\xi} P^{\mu\alpha} P^{\nu\beta} P_\alpha P_\beta\right) = \delta_{\lambda}^{\nu}, \quad (103)$$

with $\mathbf{p}^2 = -P^2 + (P \cdot u)^2$. Note that $\left(\frac{u_\mu u_\lambda}{\mathbf{p}^2} + \frac{P_{\mu\lambda}^T}{P^2} - \xi \frac{P_\mu P_\lambda}{\mathbf{p}^4}\right)$ gives the Coulomb gauge propagator at $\xi = 0$. Multiplying it to (102), we obtain

$$\begin{aligned} D_{\lambda\rho}^{<(1)} &= - \left(\frac{u_\mu u_\lambda}{\mathbf{p}^2} + \frac{P_{\mu\lambda}^T}{P^2} - \xi \frac{P_\mu P_\lambda}{\mathbf{p}^4}\right) \frac{i}{2} \left(-2P \cdot \partial g^{\mu\nu} + \partial^\mu P^\nu + \partial^\nu P^\mu - \frac{1}{\xi} P^{\mu\alpha} P^{\nu\beta}\right. \\ &\left. \times (\partial_\alpha P_\beta + \partial_\beta P_\alpha)\right) D_{\nu\rho}^{<(0)} + \left(\frac{u_\mu u_\lambda}{\mathbf{p}^2} + \frac{P_{\mu\lambda}^T}{P^2} - \xi \frac{P_\mu P_\lambda}{\mathbf{p}^4}\right) \frac{i}{2} \left(\Pi^{\mu\nu>(0)} D_{\nu\rho}^{<(0)} - \Pi^{\mu\nu<(0)} D_{\nu\rho}^{>(0)}\right). \end{aligned} \quad (104)$$

We first show terms $\propto P_{\mu\lambda}^T$ vanish by classical kinetic equations. To see that, we note $D_{\nu\rho}^{</>(0)} \propto P_{\nu\rho}^T$. The only remaining terms on the RHS are

$$\frac{P_{\mu\lambda}^T}{P^2} \frac{i}{2} \left(2P \cdot \partial g^{\mu\nu} D_{\nu\rho}^{<(0)} + \Pi^{\mu\nu>(0)} D_{\nu\rho}^{<(0)} - \Pi^{\mu\nu<(0)} D_{\nu\rho}^{>(0)}\right) \propto P_{\lambda\rho}^T. \quad (105)$$

Since the tensor structure is unique, we can extract its coefficient function by contracting with $P_T^{\lambda\rho}$, which vanishes by classical kinetic equation. The other terms give the following result in the limit $\xi \rightarrow 0$

$$\begin{aligned} D_{\lambda\rho}^{<(1)} &= -\frac{i u_\lambda (P \cdot u) \partial^\nu D_{\nu\rho}^{<(0)}}{2\mathbf{p}^2} - \frac{i P_\lambda P^{\nu\beta} \partial_\beta D_{\nu\rho}^{<(0)}}{2\mathbf{p}^2} + \frac{i u_\lambda u_\mu \left(\Pi^{\mu\nu>(0)} D_{\nu\rho}^{<(0)} - \Pi^{\mu\nu<(0)} D_{\nu\rho}^{>(0)} \right)}{2\mathbf{p}^2} \\ &= -\frac{i P_{\lambda\alpha} P^{\nu\beta} P^\alpha \partial_\beta D_{\nu\rho}^{<(0)}}{2\mathbf{p}^2} + \frac{i u_\lambda u_\mu \left(\Pi^{\mu\nu>(0)} D_{\nu\rho}^{<(0)} - \Pi^{\mu\nu<(0)} D_{\nu\rho}^{>(0)} \right)}{2\mathbf{p}^2}. \end{aligned} \quad (106)$$

In the second line, we have used $\partial^\nu D_{\nu\rho}^{<(0)} = -P^{\nu\beta} \partial_\beta D_{\nu\rho}^{<(0)}$. However, (106) cannot be the correct quantum correction to Wigner function. Since $D_{\nu\rho}^{<}$ is hermitian, a purely imaginary $D_{\nu\rho}^{<(1)}$ in (106) indicates it should be anti-symmetric in indices [66], which is obviously not satisfied by (106). The resolution is simple: since we consider on-shell photon, the operator $-P^2 g^{\mu\nu} + P^\mu P^\nu - \frac{1}{\xi} P^{\mu\alpha} P^{\nu\beta} P_\alpha P_\beta$ contains zero mode. (106) can be modified by zero mode contribution. We can make (106) hermitian by adding its own hermitian conjugate

$$D_{\lambda\rho}^{<(1)} = \frac{i P_{\rho\alpha} P^{\nu\beta} P^\alpha \partial_\beta D_{\nu\lambda}^{<(0)}}{2\mathbf{p}^2} + \frac{i u_\rho u_\mu \left(\Pi^{\mu\nu>(0)} D_{\nu\lambda}^{<(0)} - \Pi^{\mu\nu<(0)} D_{\nu\lambda}^{>(0)} \right)}{2\mathbf{p}^2}. \quad (107)$$

It turns out (107) is at the same time a zero mode of $-P^2 g^{\mu\nu} + P^\mu P^\nu - \frac{1}{\xi} P^{\mu\alpha} P^{\nu\beta} P_\alpha P_\beta$ using $D_{\nu\lambda}^{<(0)} \propto P_{\nu\lambda}^T \delta(P^2)$. Adding up (106) and (107), we find the quantum correction

$$\begin{aligned} D_{\lambda\rho}^{<(1)} &= -\frac{i P_{\lambda\alpha} P^{\nu\beta} P^\alpha \partial_\beta D_{\nu\rho}^{<(0)}}{2(-P^2 + (P \cdot u)^2)} + \frac{i u_\lambda u_\mu \left(\Pi^{\mu\nu>(0)} D_{\nu\rho}^{<(0)} - \Pi^{\mu\nu<(0)} D_{\nu\rho}^{>(0)} \right)}{2(-P^2 + (P \cdot u)^2)} - (\lambda \leftrightarrow \rho) \\ &= -2\pi\epsilon(P \cdot u) \delta(P^2) \frac{i P_{\lambda\alpha} P^{\nu\beta} P^\alpha \partial_\beta P_{\nu\rho}^T f_\gamma(P)}{2(-P^2 + (P \cdot u)^2)} + 2\pi\epsilon(P \cdot u) \delta(P^2) P_{\nu\rho}^T \times \\ &\frac{i u_\lambda u_\mu \left(\Pi^{\mu\nu>(0)} f_\gamma(P) - \Pi^{\mu\nu<(0)} (1 + f_\gamma(P)) \right)}{2(-P^2 + (P \cdot u)^2)} - (\lambda \leftrightarrow \rho). \end{aligned} \quad (108)$$

In the collisionless limit, (108) agrees with [66]. To see the equivalence, we note that counterpart in [66] can be obtained by replacing $P_{\nu\rho}^T$ in the first term by $P_{\nu\rho}$. The difference from the replacement is proportional to

$$P_{\lambda\alpha} P^\alpha P_\mu P^{\mu\beta} \partial_\beta P_{\rho\sigma} P^\sigma - (\lambda \leftrightarrow \rho), \quad (109)$$

which vanishes identically by the anti-symmetrization in indices.

Finally let us comment on the nature of the solutions (100) and (108). Both $S^{<(1)}$ and $D_{\mu\nu}^{<(1)}$ satisfy constraint equations, so they can be determined entirely from lower order solutions $S^{<(0)}$ and $D_{\mu\nu}^{<(0)}$. So (100) and (108) are referred to as non-dynamical part of the solution. In fact, (99) and (102) only determine $S^{<(1)}$ and $D_{\mu\nu}^{<(1)}$ up to possible zero

modes, which have the same form as the lowest order solutions (17) and (29), except with $f_V^{e/\gamma}$ and $f_A^{e/\gamma}$ replaced by $\delta f_V^{e/\gamma}$ and $\delta f_A^{e/\gamma}$ respectively. $\delta f_V^{e/\gamma}$ and $\delta f_A^{e/\gamma}$ can be viewed as quantum correction to distribution functions. They need to be determined from dynamical equations, which involves quantum correction to the collision term. The resulting zero modes are referred to as dynamical part of the solution. Despite our assumption of parity invariance, a non-vanishing $\delta f_A^{e/\gamma}$ may be dynamically generated when parity violating sources are present. For example δf_A^e may be generated by $\vec{a} \cdot \vec{\omega}$, with \vec{a} and $\vec{\omega}$ being fluid acceleration and vorticity respectively. It can also contribute to spin polarization at $O(\hbar)$. We leave further analysis for future studies.

6 Outlook

We have derived a quantum kinetic theory for QED by assuming parity invariance. At lowest order in \hbar , it generalizes the well-known classical kinetic theory to massive case. We have also found non-dynamical part of the quantum correction to the Wigner function at $O(\hbar)$, which gives the spin polarization of fermions and photons. Several interesting extensions of this work can be studied:

First of all, relaxing the parity invariant constraint would introduce more degrees of freedom to the kinetic theory. It makes the distribution functions spin-dependent, allowing us to study the spin evolution within kinetic theory. These are of particular interest in the physics like chiral magnetic effect, in which local parity violation is necessary.

Secondly, the notion of locality can be further explored in the kinetic theory. We have different scales for collisions with $1/e^2\Lambda$ corresponds to the effective range of inelastic collisions and $1/e\Lambda$ corresponds to the range of elastic collisions. In our case, both are local because of our larger coarse-graining scale $1/e^4\Lambda$. It would be interesting to look at other possibilities, for example, choosing $1/e\Lambda$ as coarse-graining scale would lead to non-local inelastic collisions, allowing us to study transfer between orbital and spin angular momenta. With this finer notion of locality, we also need to take into account the electromagnetic field from fluctuations.

Finally it is clearly desirable to extend the present study to QCD case and determine the corresponding spin transport coefficients. This would shed light on the applicability of spin hydrodynamics in the system of spinning quark-gluon plasma produced heavy ion collisions.

7 Acknowledgments

We are grateful to Wei-jie Fu, Jian-hua Gao, Defu Hou, Shi Pu, Xin-li Sheng and Ziyue Wang for useful discussions. This work is in part supported by NSFC under Grant Nos 12075328, 11735007 and 11675274.

A From self-energies to collision term

In this appendix, we show how (41), (42), (43), (44), (45) and (46) can be reduced to collision term in Boltzmann equation for QED.

We start with (41) and focus on the case $p_0 > 0$, i.e. fermion in the initial state. The case $p_0 < 0$ can be deduced by crossing symmetry. There are in total 8 ways in choosing the sign of k_0 , k'_0 and p'_0 . Only the following three are kinematically allowed: $k_0 > 0, k'_0 > 0, p'_0 > 0$; $k_0 < 0, k'_0 < 0, p'_0 > 0$ and $k_0 < 0, k'_0 > 0, p'_0 < 0$. The second and third cases are related to the first one by crossing symmetry. Let us consider the first case. The kinematical region implies it corresponds to square of s-channel Compton. To see that, we use

$$P_{\nu\mu}^T(K) = \sum_i \epsilon_\nu^i(K) \epsilon_\mu^{i*}(K), \quad (110)$$

and similarly for $P_{\sigma\rho}^T(K')$, which relate the projector to sum over initial/final states of photon. We can further use the spin sum formula for $\not{P} + m$ from $S^<(P)$

$$\not{P} + m = \sum_s u_s(P) \bar{u}_s(P), \quad (111)$$

and similarly for $\not{P}' + m$ from $S^>(P')$. Recall in Section.2 that trace will be taken in deriving dynamical equation for f_e . With all the rewritings above and cyclic property of trace, we have from $\text{tr}[(41)]^9$

$$\begin{aligned} & \sum_{s,t,i,j} \text{tr}[\bar{u}_s(P) \gamma^\mu S_{11}(K+P) \gamma^\rho u_t(P') \epsilon_\sigma^i(K') \epsilon_\mu^j(K) \bar{u}_t(P') \gamma^\sigma S_{22}(K+P) \gamma^\nu u_s(P) \epsilon_\rho^{i*}(K') \epsilon_\nu^{j*}(K)] \\ & \times f_e(P) f_\gamma(K) (1 - f_e(P')) (1 + f_\gamma(K')) \delta(P^2) \delta(P'^2) \delta(K^2) \delta(K'^2), \end{aligned} \quad (112)$$

which is clearly identified as square of s-channel Compton scattering. By crossing symmetry, we obtain square of t-channel Compton scattering and t-channel annihilation for the other two cases. The action of crossing symmetry on distribution functions use the constraints

⁹An overall numerical factor $(2\pi)^4$ is suppressed.

$f_e(P) + f_e(-P) = 1$ and $f_\gamma(P) + f_\gamma(-P) = 1$ to convert distribution functions of particles to that of anti-particles.

(42) can be rewritten similarly. For the case $p_0 > 0$, $k_0 > 0$, $k'_0 > 0$ and $p'_0 > 0$, we also use (110), (111) to rewrite $\text{tr}[(42)]$ as

$$\begin{aligned} & \sum_{s,t,i,j} \text{tr}[\bar{u}_s(K')\gamma^\beta u_t(P')\bar{u}_t(P')\gamma^\alpha u_s(K')]\text{tr}[\bar{u}_i(P)\gamma^\mu u_j(K)\bar{u}_j(K)\gamma^\nu u_i(P)]D_{\nu\alpha}^{11}(K-P) \times \\ & D_{\beta\mu}^{22}(K-P)f_e(P)f_e(P')(1-f_e(K))(1-f_e(K'))\delta(P^2)\delta(P'^2)\delta(K^2-m^2)\delta(K'^2-m^2), \end{aligned} \quad (113)$$

which corresponds to square of t-channel Coulomb scattering between fermions. By crossing symmetry, we can obtain also the squares of s/t-channel Coulomb scattering between fermion and anti-fermion.

Now we turn to (43). In fact, $\text{tr}[(41)]$ and (43) are simply related by relabeling of momenta $P \leftrightarrow K$. It follows that (43) also correspond to squares of s/t-channel Compton scattering and t-channel annihilation.

The identification with interference terms proceeds similarly. For vertex correction to photon self-energy (44), we can use cyclic property of trace to rewrite (44) up to overall factors of $f_\gamma(P)f_e(P')(1-f_e(K))(1+f_\gamma(K'))\delta(P^2)\delta(P'^2)\delta(K^2-m^2)\delta(K'^2-m^2)$ as

$$\begin{aligned} & \sum_{s,t,i,j} \text{tr}[\bar{u}_s(K)\gamma^\mu S_{22}(P-K)\gamma^\rho u_t(P')]\epsilon_\rho^i(Q)\epsilon_\mu^{j*}(P) \\ & \times \text{tr}[\bar{u}_t(P')\gamma^\nu S_{11}(P+P')\gamma^\sigma u_s(K)]\epsilon_\sigma^{i*}(Q)\epsilon_\nu^j(P) \\ & = \sum_{s,t,i,j} (\text{tr}[\bar{u}_t(P')\gamma^\rho S_{11}(P-K)\gamma^\mu u_s(K)]\epsilon_\rho^{i*}(Q)\epsilon_\mu^j(P))^* \\ & \times \text{tr}[\bar{u}_t(P')\gamma^\nu S_{11}(P+P')\gamma^\sigma u_s(K)]\epsilon_\sigma^{i*}(Q)\epsilon_\nu^j(P). \end{aligned} \quad (114)$$

This is the product of the s-channel amplitude with the complex conjugate of t-channel amplitude for Compton scattering, to be abbreviated st^* of Compton. By crossing symmetry, we can easily obtain the s^*t of Compton and t^*u of annihilation. Note that we have only half of the interference terms for annihilation.

For the vertex correction to fermion self-energy, we look at (45) first. Using (21), we have

$$S^>(-P') = \bar{S}^<(P'). \quad (115)$$

Note that \bar{S} has sign of mass flipped. We can represent the corresponding Dirac structure

by the spin sum of anti-fermions

$$P' - m = \sum_s v_s(P') \bar{v}_s(P'). \quad (116)$$

We can then rewrite the trace of (45) up to $f_e(P)f_e(P')(1 + f_\gamma(K))(1 + f_\gamma(K'))\delta(P^2 - m^2)\delta(P'^2 - m^2)\delta(K^2)\delta(K'^2)$ as

$$\begin{aligned} & \sum_{s,t,i,j} \text{tr}[\bar{u}_s(P)\gamma^\mu S_{22}(P-K)\gamma^\nu v_t(P')]\epsilon_\mu(K)\epsilon_\nu^*(K') \\ & \times \text{tr}[\bar{v}_t(P')\gamma^\rho S_{11}(P-K')\gamma^\sigma u_s(P)]\epsilon_\rho^*(K)\epsilon_\sigma(K') \\ & = \sum_{s,t,i,j} (\text{tr}[\bar{v}_t(P')\gamma^\nu S_{11}(P-K)\gamma^\mu u_s(P)]\epsilon_\mu^*(K)\epsilon_\nu(K'))^* \\ & \times \text{tr}[\bar{v}_t(P')\gamma^\rho S_{11}(P-K')\gamma^\sigma u_s(P)]\epsilon_\rho^*(K)\epsilon_\sigma(K'), \end{aligned} \quad (117)$$

which corresponds to half of the interference term of annihilation. By crossing symmetry, we can obtain interference terms of Compton scattering.

Finally we turn to (46), which has slightly different momenta labeling from the other cases, with P , P' , $P-K$ and $P-K'$ on-shell instead. We consider the kinematical region with $p'_0 < 0$, $p_0 - k_0 > 0$, $p_0 - k'_0 > 0$. Using similar procedure as before, we rewrite (46) up to overall factors of $f_e(P)f_e(P')(1 + f_\gamma(P-K))(1 + f_\gamma(P-K'))\delta(P^2 - m^2)\delta(P'^2 - m^2)\delta((P-K)^2 - m^2)\delta((P-K')^2 - m^2)$ as

$$\begin{aligned} & \sum_{s,t,i,j} \text{tr}[\bar{u}_s(P)\gamma^\mu u_t(P-K)]\text{tr}[\bar{u}_i(-P')\gamma^\rho u_j(P-K')]D_{\mu\rho}^{22}(K) \\ & \times \text{tr}[\bar{u}_t(P-K)\gamma^\nu u_i(-P')]\text{tr}[\bar{u}_j(P-K')\gamma^\sigma u_s(P)]D_{\nu\sigma}^{11}(K') \\ & = \sum_{s,t,i,j} (\text{tr}[\bar{u}_t(P-K)\gamma^\mu u_s(P)]\text{tr}[\bar{u}_j(P-K')\gamma^\rho u_i(-P')])D_{\mu\rho}^{11}(K))^* \\ & \times \text{tr}[\bar{u}_t(P-K)\gamma^\nu u_i(-P')]\text{tr}[\bar{u}_j(P-K')\gamma^\sigma u_s(P)]D_{\nu\sigma}^{11}(K'). \end{aligned} \quad (118)$$

This gives the product of t-channel amplitude with complex conjugate of u-channel amplitude of Coulomb scattering between fermions (tu^*). By crossing symmetry, we can also obtain st^* and s^*t of Coulomb scattering between fermion and anti-fermion.

B Evaluation of self-energies

In this appendix, we evaluate the retarded self-energy of fermions and photons, which are needed for determination of thermal masses in the main text. The retarded self-energies

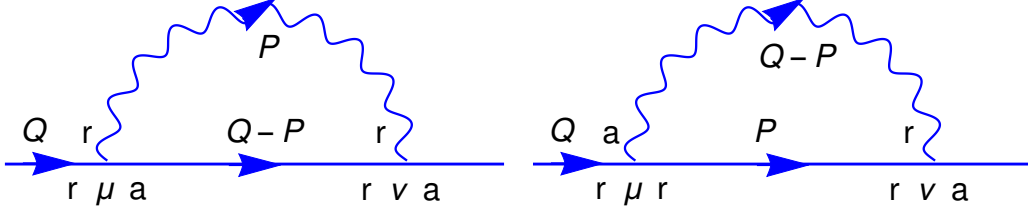


Figure 9: One-loop fermion self-energy Σ_{ra} . Vertices can have labelings rra and aaa .

have the following representation in ra basis: $S_R = iS_{ra}$ and $D_{\mu\nu}^R = iD_{\mu\nu}^{ra}$, which allows us to perform the calculation in ra basis.

We first evaluate the fermion self-energy, for which we need in two different kinematical regions: soft off-shell momenta (for screening effect in elastic collisions) and hard on-shell momenta (for inelastic collisions). In both cases, we also require $m \lesssim e\Lambda$ in order for screening or inelastic collisions to be relevant. This condition allows us to drop m in the evaluation of fermion self-energy. It is known from explicit calculations that the fermion self-energies in equilibrium are the same in Coulomb gauge [65] and Feynman gauge [78]. The agreement is expected to hold for off-equilibrium case at the lowest order because the structures of propagators do not change from equilibrium to off-equilibrium case. Below we will proceed in Feynman gauge. Fig. 9 shows the self-energy diagrams in ra basis, which give

$$\Sigma_{ra}(Q) = -e^2 \int_P \gamma^\mu S_{ar}(Q-P) \gamma^\nu D_{\nu\mu}^{rr}(P) - e^2 \int_P \gamma^\mu S_{rr}(P) \gamma^\nu D_{\nu\mu}^{ar}(Q-P). \quad (119)$$

The relevant propagators in ra basis are give by

$$\begin{aligned} S_{ar}(P) &= \frac{i(\not{P} + m)}{(p_0 - i\epsilon)^2 - p^2 - m^2}, \\ S_{rr}(P) &= \left(\frac{1}{2} - f_e(P)\right) (\not{P} + m) 2\pi\epsilon(p_0) \delta(P^2 - m^2), \\ D_{\mu\nu}^{ar}(P) &= \frac{-ig_{\mu\nu}}{(p_0 - i\epsilon)^2 - p^2}, \\ D_{\mu\nu}^{rr}(P) &= -g_{\mu\nu} \left(\frac{1}{2} + f_\gamma(P)\right) 2\pi\epsilon(p_0) \delta(P^2). \end{aligned}$$

As we argued above, we can drop m in S_{ar} and S_{rr} . Furthermore, we can drop Q^2 in the denominators of $S_{ar}(Q-P)$ and $D_{\nu\mu}^{ar}(Q-P)$, because either Q is soft off-shell $Q^2 \ll Q \cdot P$ or hard on-shell $Q^2 = 0$. We thus have

$$\begin{aligned} i\Sigma_{ra}(Q) &= -e^2 \int_P \frac{-2(Q - \not{P})}{-2P \cdot Q} \left(\frac{1}{2} + f_\gamma(P)\right) 2\pi\epsilon(p_0) \delta(P^2) \\ &\quad - e^2 \int_P \frac{-2\not{P}}{-2P \cdot Q} \left(\frac{1}{2} - f_e(P)\right) 2\pi\epsilon(p_0) \delta(P^2), \end{aligned} \quad (120)$$

where we have dropped $i\epsilon$ in the denominators because $Q - P$ is off-shell. Separating the cases of particles and anti-particles, we can expand (120) as

$$\begin{aligned}
i\Sigma_{ra}(Q) &= -e^2 \int \frac{d^3p}{(2\pi)^3} \frac{1}{2p} \left(\frac{-2(Q - \not{P})}{-2P \cdot Q} \left(\frac{1}{2} + f_\gamma(\vec{p}) \right) - \frac{-2(Q - \not{\bar{P}})}{-2\bar{P} \cdot Q} \left(\frac{1}{2} - f_\gamma(-\vec{p}) \right) \right) \\
&\quad - e^2 \int \frac{d^3p}{(2\pi)^3} \frac{1}{2p} \left(\frac{-2\not{P}}{-2P \cdot Q} \left(\frac{1}{2} - f_e(\vec{p}) \right) - \frac{-2\not{\bar{P}}}{-2\bar{P} \cdot Q} \left(-\frac{1}{2} - f_{\bar{e}}(-\vec{p}) \right) \right), \quad (121)
\end{aligned}$$

where $\bar{P} = (-p_0, \vec{p})$ and $f_{\bar{e}}$ is the distribution function of anti-fermions defined below (48).

We can then use a change a variable $\vec{p} \rightarrow -\vec{p}$ to arrive at

$$\begin{aligned}
i\Sigma_{ra}(Q) &= -e^2 \int \frac{d^3p}{(2\pi)^3} \frac{1}{2p} \left(\frac{-2(Q - \not{P})}{-2P \cdot Q} \left(\frac{1}{2} + f_\gamma(\vec{p}) \right) - \frac{-2(Q + \not{P})}{2P \cdot Q} \left(-\frac{1}{2} - f_\gamma(\vec{p}) \right) \right) \\
&\quad - e^2 \int \frac{d^3p}{(2\pi)^3} \frac{1}{2p} \left(\frac{-2\not{P}}{-2P \cdot Q} \left(\frac{1}{2} - f_e(\vec{p}) \right) - \frac{2\not{P}}{2P \cdot Q} \left(\frac{1}{2} + f_{\bar{e}}(\vec{p}) \right) \right). \quad (122)
\end{aligned}$$

Dropping the $\frac{1}{2}$ in the brackets, which correspond to the vacuum contributions, we end up with

$$i\Sigma_{ra}(Q) = e^2 \int \frac{d^3p}{(2\pi)^3} \frac{1}{2p} \frac{\not{P}}{P \cdot Q} (2f_\gamma(\vec{p}) + f_e(\vec{p}) + f_{\bar{e}}(\vec{p})). \quad (123)$$

Since we require $m \lesssim e\Lambda$ and Q can be either hard on-shell or soft off-shell, including mass in the evaluation of fermion self-energy would only lead to a correction at order $O(e^3\Lambda^2/Q)$.

Next we turn to the retarded photon self-energy, for which we also need in two different kinematical regions: soft off-shell momenta (for screening in elastic collisions) and hard on-shell momenta (for inelastic collisions). However, there is one small difference from the fermion self-energy. While in case of inelastic collisions, photon self-energy is never needed for very massive fermion $m \gg e\Lambda$ because this would make inelastic scattering itself irrelevant, it is always needed for screening in elastic collisions for arbitrary fermion mass. So we will not drop m as in the following evaluation of photon self-energy. Since the photon self-energy at leading order in coupling is gauge invariant. We can also evaluate it in Feynman gauge. The corresponding diagrams are shown in Fig. 10, which give

$$\begin{aligned}
\Pi_{\mu\nu}^{ra} &= e^2 \int_P \text{tr}[\gamma^\mu S_{rr}(P)\gamma^\nu S_{ra}(P - Q)] + e^2 \int_P \text{tr}[\gamma^\mu S_{ar}(P)\gamma^\nu S_{rr}(Q - P)] \\
&= e^2 \int_P \text{tr}[\gamma^\mu S_{rr}(P)\gamma^\nu S_{ra}(P - Q)] + (Q \rightarrow -Q, \mu \leftrightarrow \nu). \quad (124)
\end{aligned}$$

The contribution from the second diagram is related the counterpart from the first one by the replacement $Q \rightarrow -Q, \mu \leftrightarrow \nu$. This can be shown by using the property $S_{ar}(P) = S_{ra}(P)$ valid for off-shell momentum and relabeling of momentum $P \rightarrow Q - P$. Keeping fermion

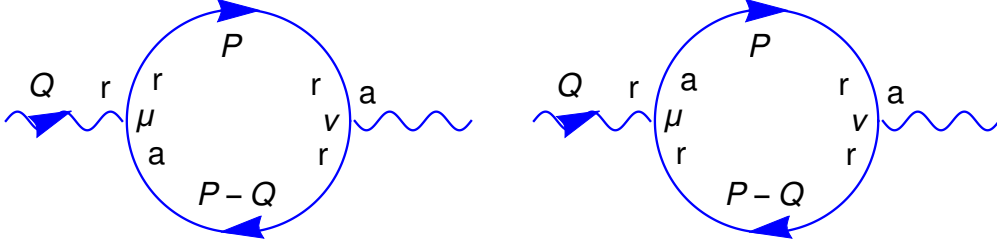


Figure 10: One-loop hard photon self-energy Π_{ra} . Vertices can have labelings rra and aaa .

mass in the propagators for the photonic case, we evaluate the trace as

$$\text{tr}[\gamma^\mu(\not{P} + m)\gamma^\nu(\not{P} - Q + m)] = 8P^\mu P^\nu - 4(P^\mu Q^\nu + P^\nu Q^\mu) + 4g^{\mu\nu}P \cdot Q. \quad (125)$$

Note that the m -dependence drops by the on-shell condition of P . The remaining evaluation is similar to the fermionic case. In the end, we find two diagrams contribute equally to give

$$i\Pi_{\mu\nu}^{ra} = 2e^2 \int \frac{d^3p}{(2\pi)^3} \frac{1}{E_p} (f_e(\vec{p}) + f_{\bar{e}}(\vec{p})) (P_\mu Q_\nu + P_\nu Q_\mu - g_{\mu\nu}P \cdot Q) \frac{1}{P \cdot Q}, \quad (126)$$

with $E_p = \sqrt{p^2 + m^2}$. The Ward identity can be verified as

$$iQ^\mu \Pi_{\mu\nu}^{ra} = 2e^2 \int \frac{d^3p}{(2\pi)^3} \frac{1}{E_p} (f_e(\vec{p}) + f_{\bar{e}}(\vec{p})) \frac{P_\nu Q^2}{P \cdot Q}, \quad (127)$$

which holds for the two kinematic regions we consider: for hard on-shell photon, it vanishes by $Q^2 = 0$ and for soft off-shell photon $Q \sim e\Lambda$, it vanishes up to the order we keep: $iQ^\mu \Pi_{\mu\nu}^{ra} \sim O(e^3\Lambda^3)$.

Finally we calculate the self-energy $\Pi_{\mu\nu}^{aa}$ for soft photon, which will be used to determine $D_{\mu\nu}^{rr}$. In this case, we also have $m \lesssim e\Lambda$ so that inelastic collisions is relevant. $\Pi_{\mu\nu}^{aa}$ contains contributions from three diagrams in Fig. 11. Only the last one is medium dependent, which gives

$$\begin{aligned} \Pi_{\mu\nu}^{aa}(Q) &= e^2 \int_{P,P'} (2\pi)^4 \delta(P - P' - Q) \text{tr}[\gamma^\mu \not{P} \gamma^\nu \not{P}'] 2\pi\epsilon(p_0)\delta(P^2) \left(\frac{1}{2} - f_e(P)\right) \\ &\quad \times 2\pi\epsilon(p'_0)\delta(P'^2) \left(\frac{1}{2} - f_e(P')\right). \end{aligned} \quad (128)$$

Note that we have dropped mass in the propagators. For $Q \ll P, P'$, p_0 and p'_0 have the same sign, thus $\epsilon(p_0)\epsilon(p'_0) = 1$. We expand the delta functions and evaluate the trace to obtain

$$\begin{aligned} \Pi_{\mu\nu}^{aa}(Q) &= e^2 \int \frac{d^3p}{(2\pi)^3} \frac{1}{4pp'} (2\pi)\delta(p - |\mathbf{p} - \mathbf{q}| - q_0) [(4P^\mu P'^\nu + 4P^\nu P'^\mu - 4g^{\mu\nu}P \cdot P') \\ &\quad \left(\frac{1}{2} - f_e(\vec{p})\right)\left(\frac{1}{2} - f_e(\vec{p}')\right) + (4\bar{P}^\mu \bar{P}'^\nu + 4\bar{P}^\nu \bar{P}'^\mu - 4g^{\mu\nu}\bar{P} \cdot \bar{P}') \left(\frac{1}{2} - f_{\bar{e}}(-\vec{p})\right)\left(\frac{1}{2} - f_{\bar{e}}(-\vec{p}')\right)]. \end{aligned} \quad (129)$$

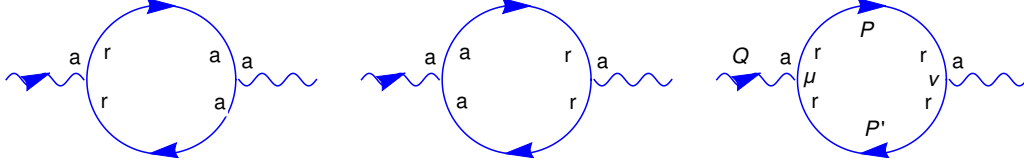


Figure 11: One-loop soft photon self-energy Π_{aa} . Vertices can have labelings rra and aaa . Only the third diagram is medium dependent.

We further approximate $P'^\mu \simeq P^\mu$, $\bar{P}'^\mu \simeq \bar{P}^\mu$ and neglect $P \cdot P' = -Q^2 + 2m^2$. Finally we make a change of variable $\vec{p} \rightarrow -\vec{p}$. It amounts to the replacement $\bar{P} \rightarrow -P$ and $f_{\bar{e}}(-\vec{p}) \rightarrow f_{\bar{e}}(\vec{p})$, after which we obtain

$$\Pi_{\mu\nu}^{aa} = e^2 \int \frac{d^3p}{(2\pi)^3} 2\hat{P}^\mu \hat{P}^\nu (2\pi) \delta(p - |\mathbf{p} - \mathbf{q}| - q_0) (f_e(\vec{p})^2 - f_{\bar{e}}(\vec{p})) + (f_e \rightarrow f_{\bar{e}}), \quad (130)$$

with $\hat{P}^\mu = (1, \hat{p})$.

To determine $D_{\mu\nu}^{rr}$, we use the following identities

$$\begin{aligned} D_{\mu\nu}^{rr} &= \frac{1}{2} (D_{\mu\nu}^> + D_{\mu\nu}^<), \\ \Pi_{\mu\nu}^{aa} &= \frac{1}{2} (\Pi_{\mu\nu}^> + \Pi_{\mu\nu}^<). \end{aligned} \quad (131)$$

Using $D_{\mu\nu}^{</>} = -D_{\mu\alpha}^R \Pi^{\alpha\beta</>} D_{\beta\nu}^A + O(\hbar)$, we obtain

$$D_{\mu\nu}^{rr} = -D_{\mu\alpha}^R \Pi_{aa}^{\alpha\beta} D_{\beta\nu}^A, \quad (132)$$

where D^R is given by (56) and D^A determined from (50).

C Damping rate of hard fermion

The damping rate Γ is determined from the dispersion $p_0 = E_p - \frac{i\Gamma}{2}$, which is the root of the following equation

$$(P_\mu - \Sigma_\mu^R)^2 - (m - \Sigma_m^R)^2 = 0, \quad (133)$$

with $\Sigma^R = \Sigma_\mu^R \gamma^\mu + \Sigma_m^R 1$. It is the same equation as (60), but now we need to find out the imaginary part of p_0 . Note that $\Sigma_\mu^R \sim e^2$ and $\Sigma_m^R = 0$ to the order of our interest. From (133), we obtain

$$\Gamma = -\frac{1}{2p_0} \text{Im}(\text{tr}[\not{P}\Sigma^R]) = -\frac{1}{2p_0} \text{Re}(\text{tr}[\not{P}\Sigma^{ra}]). \quad (134)$$

We proceed with the following representation from the left panel of Fig. 9 (with P and Q exchanged)

$$\Sigma^{ra}(P) = -e^2 \int_Q \gamma^\mu S_{ar}(P-Q) \gamma^\nu D_{\nu\mu}^{rr}(Q). \quad (135)$$

Plugging (135) into (134) and using that $D_{\mu\nu}^{rr}$ is real, we obtain

$$\text{Re}(\text{tr}[\not{P}\Sigma^{ra}]) = -e^2 \int_Q \text{Re} \left(\text{tr}[\not{P}\gamma^\mu(\not{P}-\not{Q})\gamma^\nu] \frac{i}{(p_0 - q_0 - i\epsilon)^2 - (|\mathbf{p} - \mathbf{q}|)^2 - m^2} \right) D_{\nu\mu}^{rr}(Q). \quad (136)$$

Since $Q \ll P$, we can approximate $\text{tr}[\not{P}\gamma^\mu(\not{P}-\not{Q})\gamma^\nu] \simeq 8P^\mu P^\nu$ and take the real part as

$$\begin{aligned} \text{Re} \left(\frac{i}{(p_0 - q_0 - i\epsilon)^2 - (|\mathbf{p} - \mathbf{q}|)^2 - m^2} \right) &\simeq \text{Re} \left(\frac{i}{2p_0 q_0 - 2\vec{p} \cdot \vec{q} - p_0 i\epsilon} \right) \\ &= \delta(2p_0 q_0 - 2\vec{p} \cdot \vec{q}) \epsilon(p_0) = \frac{\pi}{2p_0} \delta(q_0 - q_{\parallel}), \end{aligned} \quad (137)$$

where $q_{\parallel} = \vec{q} \cdot \hat{p}$. In the end, we have

$$\Gamma = e^2 \int \frac{d^3q}{(2\pi)^3} \hat{P}^\mu \hat{P}^\nu D_{\nu\mu}^{rr}(Q). \quad (138)$$

Since Q is soft, the suppression factor e^3 from phase space d^3q is compensated by the Bose enhanced propagator $D^{rr} \sim e^{-3}$, giving $\Gamma \sim e^2$. Such enhancement mechanism is not present in the contribution from right panel of Fig. 9, so we ignore.

D Relating four-point correlators in 12 and ra basis

The lesser and greater photon self-energies require knowledge of fermion four-point correlators in the 12 basis, while we calculate in Section 4 only one particular correlator in the ra basis. In this appendix, we establish a relation between them. The fermion four-point correlator is defined as

$$G_{ijkl}(x, x', y, y') = \langle \psi_i(x) \bar{\psi}_k(y) \psi_l(y') \bar{\psi}_j(x') \rangle, \quad (139)$$

with labels taking values either in 12 or in ra basis. Using the basic relation between field in different basis

$$\psi_r = \frac{1}{2}(\psi_1 + \psi_2), \quad \psi_a = \psi_1 - \psi_2, \quad (140)$$

we easily obtain

$$G_{1122} = G_{rrrr} + \frac{1}{2}G_{rarr} + \frac{1}{2}G_{arrr} - \frac{1}{2}G_{rrar} - \frac{1}{2}G_{rrra} + \frac{1}{4}G_{aarr} + \frac{1}{4}G_{rraa} + \dots, \quad (141)$$

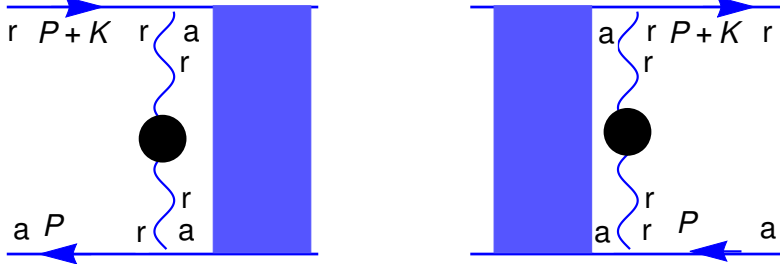


Figure 12: Labelings for G_{rarr} and G_{rrra} . By pinching mechanism, the labels are uniquely fixed. G_{arrr} and G_{rrar} can be obtained by exchanging r and a on one end. The shaded structures corresponds to G_{aarr} (left panel) and G_{rraa} (right panel) respectively.

with \dots including correlators with at least three a 's in ra basis. They are not allowed in the pinching kinematical region¹⁰. Note that we have calculated G_{aarr} . The other labelings appearing in (141) can be simply related to G_{aarr} as we now set out to find.

From the diagrammatic representations in Fig.12, we easily deduce using $S^{rr} = (S^{ra} - S^{ar}) (\frac{1}{2} - f_e)$

$$\begin{aligned}
G_{rarr} &= - \left(\frac{1}{2} - f_e(P+K) \right) G_{aarr}, \\
G_{rrra} &= \left(\frac{1}{2} - f_e(P+K) \right) G_{rraa}, \\
G_{arrr} &= \left(\frac{1}{2} - f_e(P) \right) G_{aarr}, \\
G_{rrar} &= - \left(\frac{1}{2} - f_e(P) \right) G_{rraa},
\end{aligned} \tag{142}$$

where we have extracted relevant component of S^{rr} in arriving at the above. For example, we keep S^{ar} in G_{rarr} dropping S^{ra} because it is paired with another S_{ra} . G_{rrrr} is a little complicated. We claim contributions containing alternating propagators like $\begin{pmatrix} S_{ra}(P+K) & S_{ar}(P+K) \\ S_{ar}(P) & S_{ra}(P) \end{pmatrix}$ all vanish. We show below such contribution cancel among different diagrams. Referring to Fig. 13, we see the alternating contribution can arise from four possible subdiagrams. Extracting the proportionality function of $\begin{pmatrix} S_{ra}(P+K) & S_{ar}(P+K) \\ S_{ar}(P) & S_{ra}(P) \end{pmatrix}$, we have

$$2 \left(\frac{1}{2} - f_e(P) \right) \left(\frac{1}{2} - f_e(P+K) \right) - 2 \left(\frac{1}{2} - f_e(P) \right) \left(\frac{1}{2} - f_e(P+K) \right) = 0. \tag{143}$$

Therefore only non-alternating contributions are allowed, which are either G_{aarr} or

¹⁰This is because in these cases at least one end is labeled by two a 's, then the opposite end is forced to have two r 's, contradicting the assumed number of a 's.

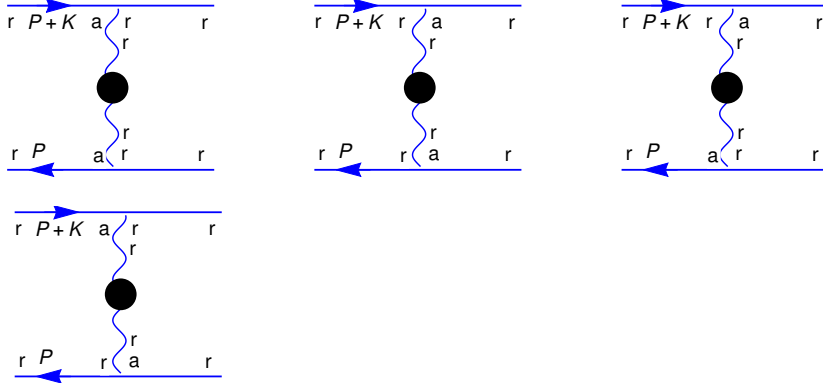


Figure 13: Possible subdiagrams contributing to alternating unit $\begin{pmatrix} S_{ra}(P+K) & S_{ar}(P+K) \\ S_{ar}(P) & S_{ra}(P) \end{pmatrix}$. Note that the labels for the part extending from both sides of the subdiagrams are uniquely fixed.

G_{rraa} . It follows

$$\begin{aligned} G_{rrrr} &= -\left(\frac{1}{2} - f_e(P)\right) \left(\frac{1}{2} - f_e(P+K)\right) (G_{aarr} + G_{rraa}) \\ &= -\left(\frac{1}{2} - f_e(P)\right) \left(\frac{1}{2} - f_e(P+K)\right) 2\text{Re}(G_{rraa}), \end{aligned} \quad (144)$$

where we have used $G_{rraa} = G_{aarr}^*$. Similar analysis gives

$$G_{2211} = f_e(P)(1 - f_e(P+K))2\text{Re}G_{aarr}. \quad (145)$$

They are off-equilibrium generalization of KMS relations in [79] in the special pinching kinematical region.

E Fermion self-energies with both vertices resummed

In this appendix, we show fermion self-energy with both vertices resummed is not allowed. We work in the ra basis. Recall from the previous appendix that all the non-vanishing four point correlators can be generated from the two basic ones G_{aarr} and G_{rraa} by flipping labels from a to r . We show in Fig. 14 three inequivalent diagrams with two vertices constructed using G_{aarr} and G_{rraa} . Other diagrams can be generated from them by flipping labels. Since labels can only be flipped from a to r , we find diagrams in the top row and those with labels flipped always contain at least an aa propagator for either fermion or photon, thus are not allowed. In the bottom row, we do find a possible flipping without aa propagators. However, this diagram contains the pair of propagators $S_{ar}(P+K)D_{ar}^{\mu\nu}(K) \sim D_{ar}(P+K)D_{ar}(K)$, which vanishes identically upon integration of k_0 by closing the contour properly.

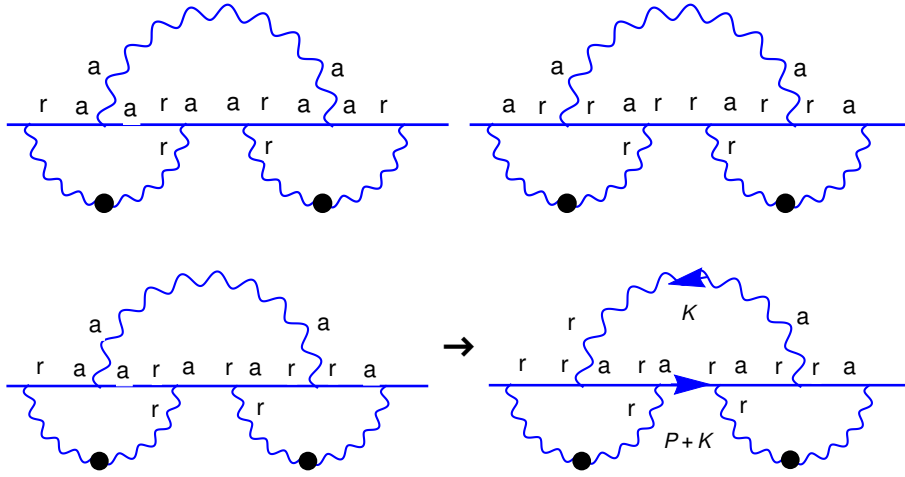


Figure 14: The top row shows self-energy diagrams with both vertices constructed from G_{rraa} or G_{aarr} . These diagrams contain one aa fermion propagator and one aa photon propagator. By flipping labels in G_{rraa} or G_{aarr} , There is always one remaining aa propagator. The bottom row shows a self-energy diagram with vertices constructed from G_{rraa} and G_{aarr} on the left. A possible flipping without aa propagator is shown on the right, which vanishes upon integration of k_0 . Multiple soft photon exchanges are allowed on each vertex. Only the outermost one is shown for clarity.

References

- [1] L. Adamczyk et al. Global Λ hyperon polarization in nuclear collisions: evidence for the most vortical fluid. *Nature*, 548:62–65, 2017.
- [2] Jaroslav Adam et al. Global polarization of Λ hyperons in Au+Au collisions at $\sqrt{s_{NN}} = 200$ GeV. *Phys. Rev. C*, 98:014910, 2018.
- [3] Jaroslav Adam et al. Polarization of Λ ($\bar{\Lambda}$) hyperons along the beam direction in Au+Au collisions at $\sqrt{s_{NN}} = 200$ GeV. *Phys. Rev. Lett.*, 123(13):132301, 2019.
- [4] D. Kobayashi, T. Yoshikawa, M. Matsuo, R. Iguchi, S. Maekawa, E. Saitoh, and Y. Nozaki. Spin current generation using a surface acoustic wave generated via spin-rotation coupling. *Phys. Rev. Lett.*, 119:077202, Aug 2017.
- [5] Mamoru Matsuo, Jun’ichi Ieda, Kazuya Harii, Eiji Saitoh, and Sadamichi Maekawa. Mechanical generation of spin current by spin-rotation coupling. *Phys. Rev. B*, 87:180402, May 2013.
- [6] Max A. Metlitski and Ariel R. Zhitnitsky. Anomalous axion interactions and topological currents in dense matter. *Phys. Rev. D*, 72:045011, 2005.
- [7] D. T. Son and Ariel R. Zhitnitsky. Quantum anomalies in dense matter. *Phys. Rev. D*, 70:074018, 2004.
- [8] Johanna Erdmenger, Michael Haack, Matthias Kaminski, and Amos Yarom. Fluid dynamics of R-charged black holes. *JHEP*, 01:055, 2009.
- [9] Nabamita Banerjee, Jyotirmoy Bhattacharya, Sayantani Bhattacharyya, Suvankar Dutta, R. Loganayagam, and P. Surowka. Hydrodynamics from charged black branes. *JHEP*, 01:094, 2011.
- [10] Yasha Neiman and Yaron Oz. Relativistic Hydrodynamics with General Anomalous Charges. *JHEP*, 03:023, 2011.
- [11] Karl Landsteiner, Eugenio Megias, and Francisco Pena-Benitez. Gravitational Anomaly and Transport. *Phys. Rev. Lett.*, 107:021601, 2011.
- [12] Koichi Hattori, Yoshimasa Hidaka, and Di-Lun Yang. Axial Kinetic Theory and Spin Transport for Fermions with Arbitrary Mass. *Phys. Rev. D*, 100(9):096011, 2019.

- [13] Nora Weickgenannt, Xin-Li Sheng, Enrico Speranza, Qun Wang, and Dirk H. Rischke. Kinetic theory for massive spin-1/2 particles from the Wigner-function formalism. *Phys. Rev. D*, 100(5):056018, 2019.
- [14] Jian-Hua Gao and Zuo-Tang Liang. Relativistic Quantum Kinetic Theory for Massive Fermions and Spin Effects. *Phys. Rev. D*, 100(5):056021, 2019.
- [15] Yu-Chen Liu, Kazuya Mameda, and Xu-Guang Huang. Covariant Spin Kinetic Theory I: Collisionless Limit. *Chin. Phys. C*, 44(9):094101, 2020. [Erratum: *Chin.Phys.C* 45, 089001 (2021)].
- [16] Xingyu Guo. Massless Limit of Transport Theory for Massive Fermions. *Chin. Phys. C*, 44(10):104106, 2020.
- [17] Dam Thanh Son and Naoki Yamamoto. Berry Curvature, Triangle Anomalies, and the Chiral Magnetic Effect in Fermi Liquids. *Phys. Rev. Lett.*, 109:181602, 2012.
- [18] Dam Thanh Son and Naoki Yamamoto. Kinetic theory with Berry curvature from quantum field theories. *Phys. Rev. D*, 87(8):085016, 2013.
- [19] M. A. Stephanov and Y. Yin. Chiral Kinetic Theory. *Phys. Rev. Lett.*, 109:162001, 2012.
- [20] Shi Pu, Jian-hua Gao, and Qun Wang. A consistent description of kinetic equation with triangle anomaly. *Phys. Rev. D*, 83:094017, 2011.
- [21] Jiunn-Wei Chen, Shi Pu, Qun Wang, and Xin-Nian Wang. Berry Curvature and Four-Dimensional Monopoles in the Relativistic Chiral Kinetic Equation. *Phys. Rev. Lett.*, 110(26):262301, 2013.
- [22] Yoshimasa Hidaka, Shi Pu, and Di-Lun Yang. Relativistic Chiral Kinetic Theory from Quantum Field Theories. *Phys. Rev. D*, 95(9):091901, 2017.
- [23] Cristina Manuel and Juan M. Torres-Rincon. Kinetic theory of chiral relativistic plasmas and energy density of their gauge collective excitations. *Phys. Rev. D*, 89(9):096002, 2014.
- [24] Cristina Manuel and Juan M. Torres-Rincon. Chiral transport equation from the quantum Dirac Hamiltonian and the on-shell effective field theory. *Phys. Rev. D*, 90(7):076007, 2014.

- [25] Anping Huang, Shuzhe Shi, Yin Jiang, Jinfeng Liao, and Pengfei Zhuang. Complete and Consistent Chiral Transport from Wigner Function Formalism. *Phys. Rev. D*, 98(3):036010, 2018.
- [26] Stefano Carignano, Cristina Manuel, and Juan M. Torres-Rincon. Consistent relativistic chiral kinetic theory: A derivation from on-shell effective field theory. *Phys. Rev. D*, 98(7):076005, 2018.
- [27] Jian-Hua Gao, Zuo-Tang Liang, Qun Wang, and Xin-Nian Wang. Disentangling covariant Wigner functions for chiral fermions. *Phys. Rev. D*, 98(3):036019, 2018.
- [28] Ziyue Wang, Xingyu Guo, Shuzhe Shi, and Pengfei Zhuang. Mass Correction to Chiral Kinetic Equations. *Phys. Rev. D*, 100(1):014015, 2019.
- [29] Shu Lin and Aradhya Shukla. Chiral Kinetic Theory from Effective Field Theory Revisited. *JHEP*, 06:060, 2019.
- [30] Jian-Hua Gao, Zuo-Tang Liang, and Qun Wang. Dirac sea and chiral anomaly in the quantum kinetic theory. *Phys. Rev. D*, 101(9):096015, 2020.
- [31] Tomoya Hayata, Yoshimasa Hidaka, and Kazuya Mameda. Second order chiral kinetic theory under gravity and antiparallel charge-energy flow. *JHEP*, 05:023, 2021.
- [32] Shi-Zheng Yang, Jian-Hua Gao, Zuo-Tang Liang, and Qun Wang. Second-order charge currents and stress tensor in a chiral system. *Phys. Rev. D*, 102(11):116024, 2020.
- [33] Shu Lin and Lixin Yang. Chiral kinetic theory from Landau level basis. *Phys. Rev. D*, 101(3):034006, 2020.
- [34] Shu Lin and Lixin Yang. Magneto-vortical effect in strong magnetic field. *JHEP*, 06:054, 2021.
- [35] Xiao-Li Luo and Jian-Hua Gao. Covariant Chiral Kinetic Equation in Non-Abelian Gauge field from "covariant gradient expansion". 7 2021.
- [36] Peter Brockway Arnold, Guy D. Moore, and Laurence G. Yaffe. Effective kinetic theory for high temperature gauge theories. *JHEP*, 01:030, 2003.
- [37] Peter Brockway Arnold, Guy D. Moore, and Laurence G. Yaffe. Transport coefficients in high temperature gauge theories. 1. Leading log results. *JHEP*, 11:001, 2000.

- [38] Peter Brockway Arnold, Guy D Moore, and Laurence G. Yaffe. Transport coefficients in high temperature gauge theories. 2. Beyond leading log. *JHEP*, 05:051, 2003.
- [39] Jun-jie Zhang, Ren-hong Fang, Qun Wang, and Xin-Nian Wang. A microscopic description for polarization in particle scatterings. *Phys. Rev. C*, 100(6):064904, 2019.
- [40] Shiyong Li and Ho-Ung Yee. Quantum Kinetic Theory of Spin Polarization of Massive Quarks in Perturbative QCD: Leading Log. *Phys. Rev. D*, 100(5):056022, 2019.
- [41] Stefano Carignano, Cristina Manuel, and Juan M. Torres-Rincon. Chiral kinetic theory from the on-shell effective field theory: Derivation of collision terms. *Phys. Rev. D*, 102(1):016003, 2020.
- [42] Di-Lun Yang, Koichi Hattori, and Yoshimasa Hidaka. Effective quantum kinetic theory for spin transport of fermions with collisional effects. *JHEP*, 07:070, 2020.
- [43] Ziyue Wang, Xingyu Guo, and Pengfei Zhuang. Local Equilibrium Spin Distribution From Detailed Balance. 9 2020.
- [44] Shuzhe Shi, Charles Gale, and Sangyong Jeon. From chiral kinetic theory to relativistic viscous spin hydrodynamics. *Phys. Rev. C*, 103(4):044906, 2021.
- [45] Nora Weickgenannt, Enrico Speranza, Xin-li Sheng, Qun Wang, and Dirk H. Rischke. Generating Spin Polarization from Vorticity through Nonlocal Collisions. *Phys. Rev. Lett.*, 127(5):052301, 2021.
- [46] Defu Hou and Shu Lin. Polarization Rotation of Chiral Fermions in Vortical Fluid. *Phys. Lett. B*, 818:136386, 2021.
- [47] Naoki Yamamoto and Di-Lun Yang. Chiral Radiation Transport Theory of Neutrinos. *Astrophys. J.*, 895(1):56, 2020.
- [48] Nora Weickgenannt, Enrico Speranza, Xin-li Sheng, Qun Wang, and Dirk H. Rischke. Derivation of the nonlocal collision term in the relativistic Boltzmann equation for massive spin-1/2 particles from quantum field theory. *Phys. Rev. D*, 104(1):016022, 2021.
- [49] Xin-Li Sheng, Nora Weickgenannt, Enrico Speranza, Dirk H. Rischke, and Qun Wang. From Kadanoff-Baym to Boltzmann equations for massive spin-1/2 fermions. *Phys. Rev. D*, 104(1):016029, 2021.

- [50] Ziyue Wang and Pengfei Zhuang. Damping and polarization rates in near equilibrium state. 5 2021.
- [51] Wojciech Florkowski, Bengt Friman, Amaresh Jaiswal, and Enrico Speranza. Relativistic fluid dynamics with spin. *Phys. Rev. C*, 97(4):041901, 2018.
- [52] David Montenegro, Leonardo Tinti, and Giorgio Torrieri. Ideal relativistic fluid limit for a medium with polarization. *Phys. Rev. D*, 96(5):056012, 2017. [Addendum: *Phys.Rev.D* 96, 079901 (2017)].
- [53] David Montenegro and Giorgio Torrieri. Causality and dissipation in relativistic polarizable fluids. *Phys. Rev. D*, 100(5):056011, 2019.
- [54] Koichi Hattori, Masaru Hongo, Xu-Guang Huang, Mamoru Matsuo, and Hidetoshi Taya. Fate of spin polarization in a relativistic fluid: An entropy-current analysis. *Phys. Lett. B*, 795:100–106, 2019.
- [55] A. D. Gallegos, U. Gürsoy, and A. Yarom. Hydrodynamics of spin currents. *SciPost Phys.*, 11:041, 2021.
- [56] Wojciech Florkowski, Avdhesh Kumar, and Radoslaw Ryblewski. Relativistic hydrodynamics for spin-polarized fluids. *Prog. Part. Nucl. Phys.*, 108:103709, 2019.
- [57] F. Becattini, Wojciech Florkowski, and Enrico Speranza. Spin tensor and its role in non-equilibrium thermodynamics. *Phys. Lett. B*, 789:419–425, 2019.
- [58] Samapan Bhadury, Wojciech Florkowski, Amaresh Jaiswal, Avdhesh Kumar, and Radoslaw Ryblewski. Relativistic dissipative spin dynamics in the relaxation time approximation. *Phys. Lett. B*, 814:136096, 2021.
- [59] Kenji Fukushima and Shi Pu. Spin hydrodynamics and symmetric energy-momentum tensors – A current induced by the spin vorticity –. *Phys. Lett. B*, 817:136346, 2021.
- [60] Shiyong Li, Mikhail A. Stephanov, and Ho-Ung Yee. Nondissipative Second-Order Transport, Spin, and Pseudogauge Transformations in Hydrodynamics. *Phys. Rev. Lett.*, 127(8):082302, 2021.
- [61] Masaru Hongo, Xu-Guang Huang, Matthias Kaminski, Mikhail Stephanov, and Ho-Ung Yee. Relativistic spin hydrodynamics with torsion and linear response theory for spin relaxation. 7 2021.

- [62] Hao-Hao Peng, Jun-Jie Zhang, Xin-Li Sheng, and Qun Wang. Ideal spin hydrodynamics from Wigner function approach. 7 2021.
- [63] Duan She, Anping Huang, Defu Hou, and Jinfeng Liao. Relativistic Viscous Hydrodynamics with Angular Momentum. 5 2021.
- [64] Peter Brockway Arnold, Dam Son, and Laurence G. Yaffe. The Hot baryon violation rate is $O(\alpha_w^5 T^4)$. *Phys. Rev. D*, 55:6264–6273, 1997.
- [65] Jean-Paul Blaizot and Edmond Iancu. The Quark gluon plasma: Collective dynamics and hard thermal loops. *Phys. Rept.*, 359:355–528, 2002.
- [66] Koichi Hattori, Yoshimasa Hidaka, Naoki Yamamoto, and Di-Lun Yang. Wigner functions and quantum kinetic theory of polarized photons. *JHEP*, 02:001, 2021.
- [67] Xu-Guang Huang, Pavel Mitkin, Andrey V. Sadofyev, and Enrico Speranza. Zilch Vortical Effect, Berry Phase, and Kinetic Theory. *JHEP*, 10:117, 2020.
- [68] Xu-Guang Huang and Andrey V. Sadofyev. Chiral Vortical Effect For An Arbitrary Spin. *JHEP*, 03:084, 2019.
- [69] Stanislaw Mrowczynski. Color filamentation in ultrarelativistic heavy ion collisions. *Phys. Lett. B*, 393:26–30, 1997.
- [70] Stanislaw Mrowczynski, Bjoern Schenke, and Michael Strickland. Color instabilities in the quark–gluon plasma. *Phys. Rept.*, 682:1–97, 2017.
- [71] Paul Romatschke and Michael Strickland. Collective modes of an anisotropic quark gluon plasma. *Phys. Rev. D*, 68:036004, 2003.
- [72] E. Petitgirard. Massive fermion dispersion relation at finite temperature. *Z. Phys. C*, 54:673–678, 1992.
- [73] Peter Brockway Arnold, Guy D. Moore, and Laurence G. Yaffe. Photon emission from ultrarelativistic plasmas. *JHEP*, 11:057, 2001.
- [74] Jing-Yuan Chen, Dam T. Son, Mikhail A. Stephanov, Ho-Ung Yee, and Yi Yin. Lorentz Invariance in Chiral Kinetic Theory. *Phys. Rev. Lett.*, 113(18):182302, 2014.
- [75] Jing-Yuan Chen, Dam T. Son, and Mikhail A. Stephanov. Collisions in Chiral Kinetic Theory. *Phys. Rev. Lett.*, 115(2):021601, 2015.

- [76] Yoshimasa Hidaka, Shi Pu, and Di-Lun Yang. Nonlinear Responses of Chiral Fluids from Kinetic Theory. *Phys. Rev. D*, 97(1):016004, 2018.
- [77] Shuai Y. F. Liu and Yi Yin. Spin polarization induced by the hydrodynamic gradients. *JHEP*, 07:188, 2021.
- [78] Michel Le Bellac. *Thermal Field Theory*. Cambridge Monographs on Mathematical Physics. Cambridge University Press, 3 2011.
- [79] Enke Wang and Ulrich W. Heinz. A Generalized fluctuation dissipation theorem for nonlinear response functions. *Phys. Rev. D*, 66:025008, 2002.